CHALMERS

Chalmers University of Technology, Sweden

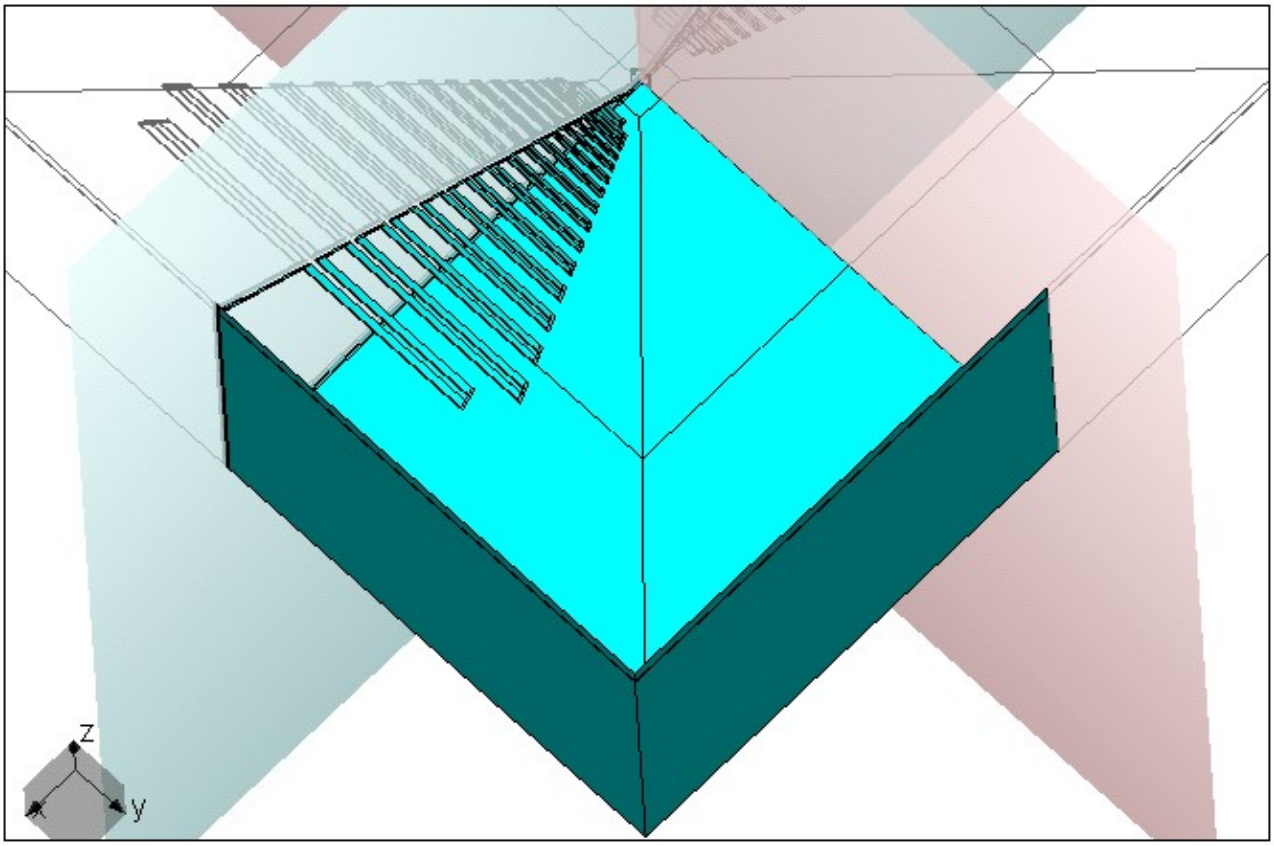

Optimization of 200-800MHz Eleven Feed for GMRT

YOGESH B. KARANDIKAR

Antenna Group
Chalmers University of Technology,
Department of Signals and Systems,
Gothenburg, Sweden 2006.

YOGESH B. KARANDIKAR

Optimization of 200-800MHz Eleven Feed for GMRT

Master Thesis at Chalmers University of Technology, Sweden.

Supervisor: Per-Simon Kildal

Antenna Group
Chalmers University of Technology,
Department of Signals and Systems,
Gothenburg, Sweden.

Gothenburg, December 2006.

Abstract

The ELEVEN feed developed by Chalmers Antenna group, is an Ultra Wide Band Feed for Reflector Antennas covering decade bandwidth. Such a feed is of interest for the Gaint Meterwave Radio Telescope (GMRT), India. This thesis discusses in depth the electrical design of the Eleven Feed for the GMRT, based on computer simulations as well as theoretical studies for understanding feed sub-efficiencies for reflector antennas of GMRT. This thesis also discusses the in depth analysis of two element dipole array as a feed for reflector in order to maximize the feed efficiency, and through analysis of two port folded dipole which is a basic element of folded dipole log periodic array used in ELEVEN feed.

Acknowledgments

First I would like to thank Prof. Govind Swarup (NCRA) who initiated the talks for Eleven Feed Design for GMRT. This initiation was then taken up by Dr. Yashawant Gupta (Chief Scientist, GMRT) & Prof. Rajaram Nityananda (Director-NCRA) with Prof. Kildal. And I am really glad that I was considered for this master thesis work by them. This was a great opportunity for me being a beginner in antenna field.

I am really happy that I had a chance to work under supervision of Prof. Kildal in his antenna group and I thank him for his guidance for understanding reflector antennas & feed sub-efficiencies.

I thank Daniel Nyberg (PhD student) for many discussions & conceptual understanding of folded dipole and for his friendship which evolved during work on two port folded dipole. I also thank Dr. Jian Yang & Prof. Jan Carlsson for many discussions about Eleven Feed modeling in WiPl-D.

Yogesh B. Karandikar

Preface

This thesis report is a master thesis for the Master's degree in Radio Astronomy & Space Science Program at Chalmers University of Technology, Göteborg, Sweden. It was conducted in Antenna Group at Chalmers under supervision of Prof. Per-Simon Kildal. Duration of the thesis work was from June 2006 to December 2006. The design specifications for this thesis work were provided by National Center for Radio Astrophysics, India considering future upgrades to GMRT system.

Being a novice in antenna field, this thesis work was certainly challenging for me with major task, to improve the reflection loss of Eleven Feed. To achieve this, efforts were taken to understand the conventional log-periodic arrays and matching techniques and then apply this to Eleven Feed. Designing a feed for world's largest interferometer-GMRT, was certainly exciting, which kept me motivating for this challenging work of Eleven Feed Design.

Finally I am solely responsible for any mistakes or errors in the thesis & suggestions are welcome to make this thesis more understandable.

Yogesh B. Karandikar
December 2006.

CONTENTS

Abstract III

Acknowledgment IV

Preface V

1. Introduction 1

2. Prime Focus Feeds for Reflectors 3
   - 2.1: Feed Pattern 3
   - 2.2: BOR1 Antennas 3
   - 2.3: Feed Sub-efficiencies 5
   - 2.4: Phase Center 6
   - 2.5: Defocussing Loss 7
   - 2.6: Total Efficiency 7
   - 2.7: Algorithm to Compute Feed Sub-efficiencies 8

3. Two Element Dipole Array as a Feed for Reflector 9
   - 3.1: Theoretical Pattern of Two Element Dipole Array with Infinite Ground Plane 9
   - 3.2: Optimum Values of DP & H to Maximize Aperture Efficiency. 12
   - 3.3: Comparisons with WiPl-D simulations 13
   - 3.4: Effect of Finite Ground Plane 16
   - 3.5: Conclusion 17

4. Conventional Log-Periodic Arrays of Dipoles 19
   - 4.1: Log-Periodic Dipole Array 19
   - 4.2: Geometrical Relations 20

5. Folded Dipole 23
   - 5.1: Conventional Folded Dipole 23
   - 5.2: Two-Port Folded Dipole 25
   - 5.3: Condition of equal Input & Load Impedance 27
   - 5.4: Results & Comparisons 27
   - 5.5: Conclusion 29

6. Folded Dipole Log-Periodic Arrays in Free Space 31
   - 6.1: Optimization Parameters 31
   - 6.2: Example of Wire FDLPA 32
   - 6.3: Conclusion 34

7. Stripe Line Studies 35

8. Plate FDLPA 37

9. Eleven Feed 39

10. Optimized Eleven Feed for GMRT 43

11. Crosspol PINs :
Innovative Concept to Reduce Crosspol 49

12. Conclusion & Further Work 53

Appendix A:
Simulation Results for Orthogonal Polarization 55
Appendix B:
Comparison between Measurements & Simulations 57

1. Introduction

Wide band antenna technologies are of growing interest in not only communication systems but also in radio astronomy with proposal of Square Kilometer Array (SKA). SKA-an international radio telescope, puts lot of challenges on engineers to achieve its design goals. One of the major challenge is to achieve one square kilometer of collecting area with enormous bandwidth of 100MHz to 25GHz.

To realize this, different antenna technologies have been considered, out of which reflector antennas with wide band feed at its focus can be considered as more promising. Olsson R. & Kildal P. S.[1] have done remarkable work to realize this with the invention of Eleven Feed which is a decade bandwidth feed for the reflector antennas, giving break thorough in wide band antenna technology.

One of the major advantage of Eleven Feed is less variation of its phase center over decade bandwidth. Eleven feed gives 11dB gain and has dimensions ~$1/11^{th}$ of the ATA feed designed for US-SKA.[2] Eleven Feed uses two parallel log periodic arrays of folded dipoles above a ground plane to give broadside radiation which is desirable to feed the reflector, while retaining the bandwidth of log periodic arrays.

Such broadband feed is of interest to Giant Meterwave Radio Telescope (GMRT), India. GMRT being world's largest interferometer at meter wavelengths gives frequency coverage of 150MHz to 1400MHz by making use of variety of feeds at its focus mounted on a faces of square cube with rotating turret.

GMRT has 30, 45m diameter parabolic reflectors operated in an interferometric array in Y-configuration. The shortest base line of 100m and longest of 26km is available. At present, GMRT observations are done in discrete frequency bands at 150, 233, 327, 610, 1420 MHz. Out of which the L-band feed is broadband from 1GHz to 1.58GHz. So obvious choice for GMRT considering the RFI scenario is the feed giving continuous frequency coverage of 200 to 800MHz.

Eleven Feed being a decade bandwidth feed for reflector, is a most suitable feed for GMRT application. So design goals of Eleven Feed for GMRT are as follows:

Table 1.1: Design Goals

Frequency Coverage:	200 to 800 MHz
Taper:	-12 dB @ 62.5^{o}
Peak Crosspolar Sidelobe:	< -15 dB
Input Reflection Coefficient:	< -11 dB
Aperture Efficiency:	> -2.2 dB
Ohmic Loss:	< 0.1 dB*

* measurement accuracy ~0.5dB with Reverberation Chamber.

At present, the Eleven Feed has S11<-6dB, so more efforts are required to achieve the goal of S11<-11dB. This will make this feed design a challenging task for this master thesis.

References:

[1] Olsson R., Kildal P.S., Weinreb S., "The Eleven Antenna: A Compact Low-Profile Decade Bandwidth Dual Polarized Feed for Reflector Antennas", IEEE Trans. Antennas & Propagation, vol. 54, No.2, February 2006.

[2] Engargiola G., "Non-planer Log-Periodic Antenna Feed for Integration with a Cryogenic Microwave Amplifier", IEEE Proceedings of Antennas & Propagation Society Symposium, pg. 140-143, June 2002.

[3] www.skatelescope.org

[4] www.gmrt.ncra.tifr.res.in

2. Prime Focus Feeds for Reflectors

Parabolic reflectors with feed at its focus is a typical setup for a radio telescope, followed by electronics for amplification and detection. Huge parabolic reflectors such as Arecibo, Greenbank, GMRT have been constructed and used for radio astronomy. Parabolic reflectors are usually characterized by their f/D ratio and surface r.m.s error. While feed for reflector is usually characterized by the term 'Aperture efficiency', which is a major of how well the feed is illuminating the parabolic dish. The aperture efficiency is further classified in various feed sub-efficiencies. Usually, the feed and the reflector are analyzed together as a transmitting system. And then same results are accepted for receiving case, due to reciprocity relations of antennas. In this section, the theory for feed efficiencies is reviewed in brief.

Ideally feed pattern should have uniform amplitude and phase of the E-field across the aperture, to have 100% aperture efficiency. But practically, the feed pattern usually has amplitude taper, side lobes, back lobes causing reduction in efficiency. Also impedance mismatch and ohmic losses in the feed, aperture blockage due to feed & support structure, surface r.m.s. errors of the dish further reduces the total efficiency of the feed and the reflector, as a transmitting or receiving system. Theory described in this section is well established by Kildal P. S. [1][2][3][4].

2.1 Feed Pattern:-

The feed pattern can be written as a sum of Copolar(CO) and Crosspolar(XP) part as follows:-

$$G(\theta,\phi)=G_{co}(\theta,\phi)\hat{co}+G_{xp}(\theta,\phi)\hat{xp} \quad .....(2.1)$$

where $\hat{co}$ = Copolar unit vector

$\hat{xp}$ = Crosspolar unit vector

If the desired polarization is along y-axis in Cartesian coordinate system then $\hat{co}=\hat{y}$ & $\hat{xp}=\hat{x}$, such that Copolar and Crosspolar unit vectors are orthogonal to each other. In spherical coordinate system, these unit vectors are written as follows:-

$$\hat{co}=\hat{y}=\sin(\phi)\hat{\theta}+\cos(\phi)\hat{\phi} \quad .....(2.2)$$

$$\hat{xp}=\hat{x}=\cos(\phi)\hat{\theta}-\sin(\phi)\hat{\phi} \quad .....(2.3)$$

Then the total radiated power can be found by evaluating the integral of radiation intensity over complete sphere.

$$P_{rad}=\frac{1}{2\eta}\iint_{4\pi}[|G_{co}(\theta,\phi)|^2+|G_{xp}(\theta,\phi)|^2]\sin(\theta)\,d\theta\,d\phi \quad ..(2.4)$$

Alternatively, the feed pattern can be expressed as

$$G(\theta,\phi)=G_{\theta}(\theta,\phi)\hat{\theta}+G_{\phi}(\theta,\phi)\hat{\phi} \quad .....(2.5)$$

This feed pattern having φ-variation of far-field can be expanded as the sum of Fourier coefficients for every theta cut.

Therefore,

$$G(\theta,\phi)=\sum_{n=0}^{n=\infty}[A_n(\theta)\sin(n\phi)+B_n(\theta)\cos(n\phi)]\hat{\theta} + \sum_{n=0}^{n=\infty}[C_n(\theta)\cos(n\phi)-D_n(\theta)\sin(n\phi)]\hat{\phi} \quad .....(2.6)$$

The minus sign in front of D_n is chosen for symmetry reasons.

If antenna is y-polarized and has two planes of symmetry in the structure then above Fourier expansion reduces to

$$G(\theta,\phi)=\sum_{n=1}^{n=\infty}[A_n(\theta)\sin(n\phi)]\hat{\theta} + \sum_{n=1}^{n=\infty}[C_n(\theta)\cos(n\phi)]\hat{\phi} \quad ....(2.7)$$

2.2 Body of Revolution Type-1 Antennas:-

In previous section, we have seen that the feed pattern can be written as the sum of Fourier series coefficients. The Body of Revolution Type-1 **(BOR1)** antennas are those whose pattern has only first order phi variations. i.e. The pattern can be completely described by only n=1 terms of the Fourier series.

Thus, BOR1 pattern can be written as,

$$G_{BOR1}(\theta,\phi)=A_1(\theta)\sin(\phi)\hat{\theta} + C_1(\theta)\cos(\phi)\hat{\phi} \quad .....(2.8)$$

Further, if the antenna is y-polarized,

$$\text{since } E-\text{plane} \rightarrow \phi=\frac{\pi}{2}, H-\text{plane} \rightarrow \phi=0$$

$$A_1(\theta)=G_E(\theta)$$

$$C_1(\theta)=G_H(\theta)$$

It can be proved[3][4] for BOR1 patterns that the Copolar and Crosspolar patterns in φ=45° plane is half the sum of and difference of E & H plane patterns respectively. Therefore,

$$G_{co45}(\theta)=\frac{1}{2}[G_E(\theta)+G_H(\theta)] \quad .....(2.9)$$

$$G_{xp45}(\theta)=\frac{1}{2}[G_E(\theta)-G_H(\theta)] \quad .....(2.10)$$

Thus, ideally if the E & H-plane patterns are same in amplitude and phase, then the cross polarization of BOR1 antenna is zero, which is very difficult to achieve practically.
Also, it can be proved[3][4] that the cross polarization of BOR1 antenna ideally excited for circular polarization is same as that of BOR1 antenna when excited ideally for linear polarization in φ=45° plane.
BOR1 patterns are important since it allow us to construct the complete pattern from E & H-plane patterns only. When the pattern for prime focus feed is considered, the BOR1 components of the pattern mainly contribute to gain on axis. So while characterizing the feeds for reflectors, first BOR1 components and BOR1 efficiency, are computed from the simulated feed patterns, which is a major of how close the feed pattern is to that of BOR1.
Computing BOR1 components, is nothing but taking n=1 term of the Fourier series expansion of the pattern. These components can be found by evaluating integrals of Fourier series as:

$$A_1(\theta)=\frac{1}{\pi}\int_{-\pi}^{\pi} G_\theta(\theta,\phi)\sin(\phi)\,d\phi \quad .....(2.11)$$

$$C_1(\theta)=\frac{1}{\pi}\int_{-\pi}^{\pi} G_\phi(\theta,\phi)\cos(\phi)\,d\phi \quad .....(2.12)$$

Once the BOR1 components are found from the feed pattern, the next step is to find BOR1 efficiency of the feed, which is defined as follows:

$$e_{BOR1}=\frac{\int_0^{\pi}[|A_1(\theta)|^2+|C_1(\theta)|^2]\sin(\theta)\,d\theta}{\sum_{n=1}^{\infty}\int_0^{\pi}[|A_n(\theta)|^2+|C_n(\theta)|^2]\sin(\theta)\,d\theta} \quad .....(2.13)$$

From the definition, it is clear that BOR1 efficiency is a ratio of power radiated by BOR1 components to the total power radiated by the feed. So the above definition can be rewritten as:

$$e_{BOR1}=\frac{\iint_{4\pi}[|BOR1_{co}(\theta,\phi)|^2+|BOR1_{xp}(\theta,\phi)|^2]\sin(\theta)\,d\theta\,d\phi}{\iint_{4\pi}[|G_{co}(\theta,\phi)|^2+|G_{xp}(\theta,\phi)|^2]\sin(\theta)\,d\theta\,d\phi} \quad .....(2.14)$$

For y-polarized antenna, BOR1 copolar and crosspolar components are computed by using equations (2.2), (2.3) & (2.8), as:

$$BOR1_{co}(\theta,\phi)=A_1(\theta)\sin^2(\phi)+C_1(\theta)\cos^2(\phi) \quad .....(2.15)$$

$$BOR1_{xp}(\theta,\phi)=\frac{1}{2}[A_1(\theta)-C_1(\theta)]\sin(2\phi) \quad .....(2.16)$$

2.3 Feed Sub-efficiencies:

After computing BOR1 components and BOR1 efficiency, all other sub-efficiencies are computed from BOR1 components only. These sub-efficiencies are spill over, illumination, polarization and phase efficiency.

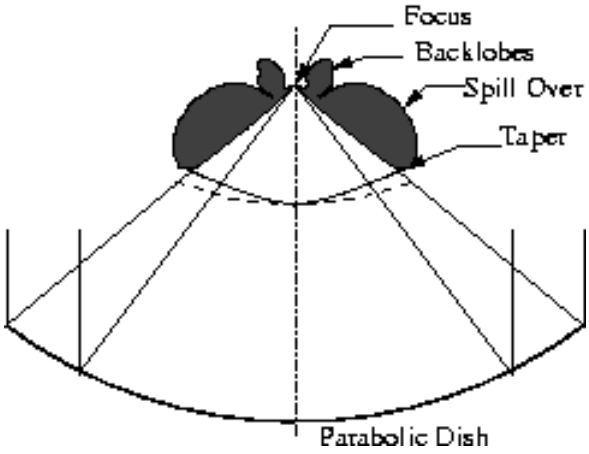

Fig 2.1: Parabolic dish & feed pattern

Spillover Efficiency:

As shown in fig 2.1, spillover efficiency represents the power loss due to radiation not hitting the reflector. Therefore its a ratio of radiated power by the feed within the subtended angle of the dish to that of total radiated power by the feed.

$$e_{sp}=\frac{2\pi\int_{0}^{\theta_o}[|G_{co45}(\theta_f)|^2+|G_{xp45}(\theta_f)|^2]\sin\theta_f\,d\theta_f}{2\pi\int_{0}^{\pi}[|G_{co45}(\theta_f)|^2+|G_{xp45}(\theta_f)|^2]\sin\theta_f\,d\theta_f} \qquad .....(2.17)$$

where

θ_o = Subtended half angle of the paraboloid

θ_f = Polar angle of feed measured w.r.t. negative z − axis

Polarization Efficiency:

This represents the power loss in the cross polarization, so its a ratio of copolar radiated power to the total radiated power with in the subtended angle of the reflector.

$$e_{pol}=\frac{\int_{0}^{\theta_o}[|G_{co45}(\theta_f)|^2]\sin\theta_f\,d\theta_f}{\int_{0}^{\theta_o}[|G_{co45}(\theta_f)|^2+|G_{xp45}(\theta_f)|^2]\sin\theta_f\,d\theta_f} \qquad .....(2.18)$$

Illumination Efficiency:

This efficiency is unity when aperture is uniformly illuminated, but practical feed patterns has taper which is a ratio of field amplitude on axis to the field amplitude at the edge of the reflector. (Higher the taper, less is the illumination efficiency) Illumination and spill over efficiencies are opposite to each other. i.e. Improving one will give adverse effect on other. So compromise is made such that the aperture efficiency is maximized.

$$e_{ill}=2\cot^2(\frac{\theta_o}{2})\frac{[\int_{0}^{\theta_o}|G_{co45}(\theta_f)|\tan(\frac{\theta_f}{2})\,d\theta_f]^2}{\int_{0}^{\theta_o}|G_{co45}(\theta_f)|^2\sin(\theta_f)\,d\theta_f} \qquad .....(2.19)$$

Phase efficiency:
This is due to non-uniform phase of the field across the aperture. It depends upon the location of the feed w.r.t focus of the reflector. To maximize the phase efficiency, the phase center of the feed pattern is computed, and then feed is located such that phase center coincides the focal point of the reflector.

$$e_{\phi}=\frac{\left|\int_0^{\theta_o} G_{co45}(\theta_f)\tan(\frac{\theta_f}{2})\,d\theta_f\right|^2}{\left[\int_0^{\theta_o}|G_{co45}(\theta_f)|\tan(\frac{\theta_f}{2})\,d\theta_f\right]^2} \quad .....(2.20)$$

Aperture Efficiency:
The aperture efficiency is nothing but the product of all feed sub-efficiencies. This describes how well the radiated power from the feed is coupled to the reflector. Practically aperture efficiency can be made as high as 70-75%.

$$e_{ap}=e_{BOR1}\cdot e_{sp}\cdot e_{pol}\cdot e_{ill}\cdot e_{\phi} \quad .....(2.21)$$

2.4 Phase Center:
Phase center is nothing but a phase reference point which reduces the variation of phase of radiated copolar field over the aperture (i.e. Parabolic dish in this context). Phase center is determined approximately for desired angular region, such that phase variations are minimized. For reflectors, this angular region is from axis to the edge of the dish i.e. $0<\theta<\theta_o$ It is defined approximately as:

$$\frac{z_{pc}}{\lambda}=\frac{\Phi_{co}(0,\phi_o)-\Phi_{co}(\theta_o,\phi_o)}{360^o(1-\cos\theta_o)} \quad .....(2.22)$$

where
$\Phi_{co}(\theta,\phi_o)=$ Phase of the copolar radiation field (degrees)
Once BOR1 components are determined from the feed pattern, then BOR1 copolar component in $\phi_o=45^o$ plane is used to find the approximate phase center by using eq. (2.22).

For parabolic reflectors, phase center is the phase reference point which maximizes the phase efficiency. If we assume small phase errors over the aperture i.e. $\Phi_{co}(\theta_o)-\Phi_{co}(0)\ll\frac{\pi}{2}$
Kildal P.S.[1][4] describes the method to obtain the location of phase center, which maximizes the phase efficiency for which we have to evaluate following six integrals.

$$I_w=\int_0^{\theta_o} w(\theta)\,d\theta \quad .....(2.23)$$

$$I_{wc}=\int_0^{\theta_o} w(\theta)[\cos(\theta)-1]\,d\theta \quad .....(2.24)$$

$$I_{wc2}=\int_0^{\theta_o} w(\theta)[\cos(\theta)-1]^2\,d\theta \quad .....(2.25)$$

$$I_{w\phi}=\int_0^{\theta_o} w(\theta)[\Phi(\theta)-\Phi(0)]\,d\theta \quad .....(2.26)$$

$$I_{w\phi 2}=\int_0^{\theta_o} w(\theta)[\Phi(\theta)-\Phi(0)]^2\,d\theta \quad .....(2.27)$$

$$I_{w\phi c}=\int_0^{\theta_o} w(\theta)[\cos(\theta)-1][\Phi(\theta)-\Phi(0)]\,d\theta \quad .....(2.28)$$

where

$$w(\theta)=|G_{co45}(\theta)|\tan(\frac{\theta}{2}) \text{ , known as weight function} \quad ...(2.29)$$

From these integrals the phase center and corresponding maximum phase efficiency is defined as:

$$(e_{\phi\delta_o})_{max} = c + \frac{b^2}{a} \quad .....(2.30)$$

$$\delta_o = \frac{1}{k} \cdot \frac{b}{a} \quad .....(2.31)$$

where

δ_o = Phase center

$(e_{\phi\delta_o})_{max}$ = maximum phase efficiency $k = \frac{2\pi}{\lambda}$

$$a = \frac{I_{wc2}}{I_w} - \left(\frac{I_{wc}}{I_w}\right)^2 \quad .....(2.32)$$

$$b = \frac{I_{w\phi c}}{I_w} - \frac{I_{w\phi} I_{wc}}{I_w^2} \quad .....(2.33)$$

$$c = 1 - \frac{I_{w\phi 2}}{I_w} + \left(\frac{I_{w\phi}}{I_w}\right)^2 \quad .....(2.34)$$

2.5 Defocussing Loss:

Practically, not always the phase center coincides the focal point of the reflector. This causes the degradation of maximum phase efficiency, due to defocussing. These small axial displacements of the phase center from the focal point reduces the maximum phase efficiency. If axial displacement δ is known from the phase center at δ_o , then degraded phase efficiency is written as:

$$e_{\phi\delta} = (e_{\phi\delta_o})_{max} - a \cdot [k(\delta - \delta_o)]^2 \quad .....(2.35)$$

The above equation can be used either to find the degraded phase efficiency if the displacement of phase center from the focal point is know or to find tolerable displacements of the phase center which reduces the maximum phase efficiency within the acceptable limits. (say 0.1dB)

For broadband feeds , there exists small variations of phase center with frequency. So its important to compute degraded phase efficiency for every frequency point of interest, since its practically not possible to place a feed with its phase center at focus of the dish for all frequencies simultaneously. It is practical to place feed with its phase center at focus for higher frequencies, since these phase center variations has comparatively less effect on longer wavelengths.

With this analysis, the aperture efficiency can be redefined as

$$e_{ap} = e_{BOR1} \cdot e_{sp} \cdot e_{pol} \cdot e_{ill} \cdot e_{\phi\delta} \quad .....(2.36)$$

2.6 Total Efficiency:

Apart from the aperture efficiency, power loss also occurs due to impedance mismatch between feed and electronic circuitry and ohmic loss in the feed due to finite conductivity of metal parts and losses in dielectric parts.

Reflection efficiency which is a major of amount of power lost due to reflections, is defined as:

$$e_r = 1 - |\Gamma|^2 \quad .....(2.37)$$

where

$\Gamma = \frac{Z_A - Z_o}{Z_A + Z_o}$ i.e. Input reflection coefficient

Z_A = Antenna Impedance

Z_o = Characteristic Impedance of transmission line

Hence Total efficiency is defined as product of all efficiencies.

$$e_{ap} = e_{BOR1} \cdot e_{sp} \cdot e_{pol} \cdot e_{ill} \cdot e_{\phi\delta} \cdot e_r \cdot e_{ohmic} \quad .....(2.38)$$

Total efficiency represents the actual amount of power transferred from the electronic circuitry to the reflector.

2.7 Algorithm to compute Feed sub-efficiencies:

1. Express feed pattern in θ,φ components. eq. (2.5)
2. Get BOR1 components from feed pattern. eq. (2.11),(2.12)
3. compute BOR1 efficiency. eq. (2.14),(2.15),(2.16)
4. Compute copolar and crosspolar BOR1 components in $\varphi=45^{o}$ plane. eq. (2.9),(2.10),(2.15),(2.16)
5. Compute spill over, polarization and illumination efficiency from these components. eq. (2.17),(2.18),(2.19)
6. Compute phase efficiency integrals. eq. (2.23) to (2.29)
7. Compute maximum phase efficiency and phase center. eq. (2.30) to (2.34)
8. For broadband feeds, compute optimum phase center for all frequencies, which could be average of all phase centers, such that defocussing loss it minimized.
9. Compute degraded phase efficiency due to small variations in phase center with frequency. eq. (2.35)
10. Compute aperture efficiency, which is product of all sub efficiencies. eq. (2.36)
11. Include reflection loss due to impedance mismatch and ohmic loss in the aperture efficiency, to get total efficiency. eq. (2.37),(2.38)

Note:- If the phase errors over the aperture are greater than π/2, it is better to first compute approximate phase center by using eq. (2.22). Then transform the phase reference point to the approximate phase center $Z_{pc.}$ And then follow the algorithm from step 6 onwards.

References:

[1] Kildal P.S., "Combined E- and H-plane phase centers of antenna feeds", IEEE Trans. Antenna & Propagation, Vol. AP-31, No. 1, January 1983.

[2] Kildal P.S., "Comments on Phase center calculations of reflector antenna feeds", IEEE Trans. Antenna & Propagation, Vol. AP-33, No. 5, May 1985.

[3] Kildal P.S., "Factorization of the feed efficiency of paraboloids and Cassegrain antennas", IEEE Trans. Antenna & Propagation, Vol. AP-33, No. 8, August 1985.

[4] Kildal P.S., "Foundations of Antennas- A Unified Approach", Studentlitteratur, 2000.

3. Two-Element Dipole Array as Feed for Reflector

An array of two half wavelength dipoles above ground plane can give broadside radiation pattern when both dipoles are excited with equal amplitude and phase. Such an array can be used as a feed for the reflector when infinite ground plane is replaced by finite one. The finite ground plane causes the scattering of the radiation emitted by dipoles near the edges, causing back lobes which reduces the aperture efficiency. In this section, such two element array with infinite ground plane has been analyzed in depth. And then effect of ground plane is studied by numerical simulations in WiPl-D software.

3.1 Theoretical Pattern of Two-element array with infinite ground plane:

The two-element dipole array on infinite ground plane as shown in fig 3.1 can be fully defined by three variables as:

1. Length of the dipole(L)
2. Separation between two dipoles(DP)
3. Height of the dipoles above ground plane(H).

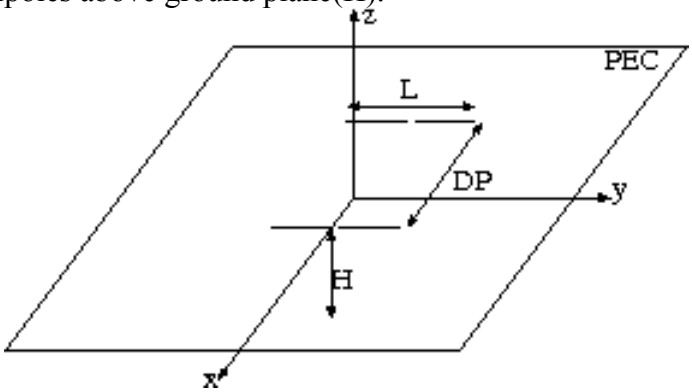

Fig 3.1 Two element dipole array

With L,DP & H defining the geometry of the array over infinite ground plane, complete far-field function of the array can be written as:

$$G(\theta,\phi)=C\cdot AF(\theta,\phi)\cdot GPF(\theta,\phi)\cdot\tilde{j}(\theta,\phi)\cdot ISF(\theta,\phi).....(3.1)$$

where

$C=$ Constant

$AF(\theta,\phi)=$ Array Factor

$GPF(\theta,\phi)=$ Ground Plane Factor

$\tilde{j}(\theta,\phi)=$ Fourier Transform of the current distribution on dipole

$ISF(\theta,\phi)=$ Incremental Source Factor

3.1.1 Incremental Source Factor:

The incremental sources can be of three types; electric, magnetic and Huygens Source. For dipoles having current distribution on them, electric current source is used. If the dipoles of the array are y-polarized as shown in fig 3.1 then far-field function of the electrical incremental source for dipoles can be written as:

$$ISF(\theta,\phi)=C_k\cdot\eta\cdot I_o\cdot[\cos(\theta)\sin(\phi)\hat{\theta}+\cos(\phi)\hat{\phi}] \quad .....(3.2)$$

where

$$C_k=\frac{-j\cdot k}{4\pi}$$

$\eta=120\pi=$ free space wave impedance.

Pattern defined in eq. (3.2) is of the type BOR1, since it has only first order phi variation. This pattern is plotted in 3-D in the fig 3.2 .

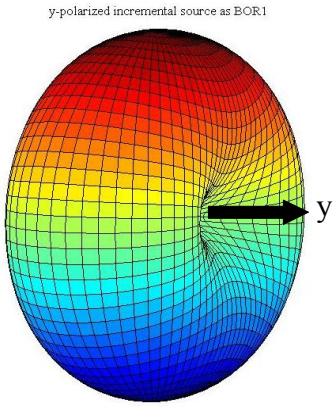

Fig 3.2: 3-D pattern of y-polarized incremental source

3.1.2 Element Pattern:

The far-field function of the finite length dipole depends upon its length and current distribution on it. If sinusoidal current distribution is assumed along the length of the dipole then the dipole pattern can be written as:

$$G_d(\hat{r}) = \tilde{j}(k\hat{l}\cdot\hat{r})\cdot G_{id}(\hat{r}) \qquad .....(3.3)$$

where

$G_{id}(\hat{r}) = \text{far}-\text{field function of incremental dipole}$

$$\tilde{j}(k\hat{l}\cdot\hat{r}) = \frac{2}{k}\frac{[\cos(k\cdot l\cdot\hat{l}\cdot\hat{r}/2)-\cos(k\cdot l/2)]}{[1-(\hat{l}\cdot\hat{r})^2]\cdot\sin(k\cdot l/2)} \qquad .....(3.4)$$

$= \text{Fourier Transform of the current distribution on dipole}$

If the dipole is y-polarized, and its length is half wavelength then $l = \frac{\lambda}{2}, \hat{l} = \hat{y} \rightarrow \hat{l}\cdot\hat{r} = \hat{y}\cdot\hat{r} = \sin(\theta)\sin(\phi)$ also $\frac{k\cdot l}{2} = \frac{\pi}{2}$

Therefore, the Fourier transform of the current distribution can be written as a function of θ,φ as follows:

$$\tilde{j}(\theta,\phi) = \frac{2}{k}\frac{\cos[\frac{\pi}{2}\sin\theta\sin\phi]}{[1-(\sin\theta\sin\phi)^2]} \qquad .....(3.5)$$

3.1.3 Ground Plane Factor:

For horizontal y-polarized dipole above infinite ground plane, the ground plane factor is written as:

$$GPF(\theta,\phi) = 2\cdot j\cdot\sin(k\cdot H\cdot\cos\theta) \qquad .....(3.6)$$

3.1.4 Array Factor:

Array Factor with element by element sum method can be written as:

$$AF(\hat{r}) = \sum_{n=1}^{N} A_n e^{j\phi_n} e^{jkr_n\cdot\hat{r}} \qquad .....(3.7)$$

where

$A_n = \text{amplitude of excitation of } n^{th} \text{ element}$

$\phi_n = \text{phase of the excitation of } n^{th} \text{ element}$

$r_n = \text{vector pointing towards the element position}$

For 2 element y-polarized dipole array as shown in fig 3.3,

N=2,

L=N*DP = 2*DP i.e. Length of the array

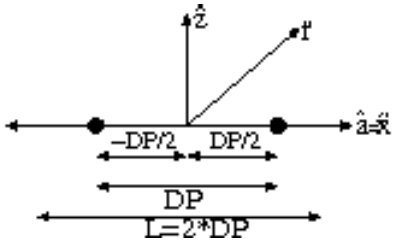

Fig 3.3: Array Geometry

If the origin of the coordinate system is chosen such that it is at the center of the two elements then

$r_1 = -DP/2\,\hat{x}$

$r_2 = DP/2\,\hat{x}$

Therefore, the array factor can be written as

$$AF(\hat{r}) = A_1 e^{j\phi_1} e^{jk(\frac{-DP}{2})\hat{x}\cdot\hat{r}} + A_2 e^{j\phi_2} e^{jk(\frac{DP}{2})\hat{x}\cdot\hat{r}} \qquad .....(3.8)$$

For broadside pattern, both elements should have equal amplitude and equal phase. Therefore, $A_1 = A_2, \phi_1 = \phi_2$

So the above equation reduces to,

$$AF(\hat{r}) = e^{jk(\frac{-DP}{2})\hat{x}\cdot\hat{r}} + e^{jk(\frac{DP}{2})\hat{x}\cdot\hat{r}}$$

$$\text{now}, \hat{x}\cdot\hat{r} = \sin\theta\cos\phi$$

$$AF(\theta,\phi) = e^{jk(\frac{-DP}{2})\sin\theta\cos\phi} + e^{jk(\frac{DP}{2})\sin\theta\cos\phi}$$

$$AF(\theta,\phi) = 2\cos[k\frac{DP}{2}\sin\theta\cos\phi] \qquad .....(3.9)$$

3.1.5 Normalized far-field function of array:

By using eq. (3.1),(3.2),(3.5),(3.6) & (3.9) the total far-field function is written as:

$$G(\theta,\phi) = 2\cos\theta[k\frac{DP}{2}\sin\theta\sin\phi]\cdot 2j\sin(kH\cos\theta)$$

$$\frac{2}{k}\frac{\cos[\frac{\pi}{2}\sin\theta\sin\phi]}{[1-(\sin\theta\sin\phi)^2]}\cdot C_k\,\eta\,I_o[\cos\theta\sin\phi\,\hat{\theta}+\cos\phi\,\hat{\phi}] \qquad .....(3.10)$$

If we express DP and H in terms of wavelength units,

$$kH \rightarrow \frac{2\pi}{\lambda}H(\lambda) \rightarrow 2\pi H$$

$$k\frac{DP}{2} \rightarrow \frac{2\pi}{\lambda}\frac{DP(\lambda)}{2} \rightarrow \pi DP$$

Substituting this in eq.(3.10), we get total far-field function of the two element array as:

$$G(\theta,\phi) = C\cdot AF(\theta,\phi)\cdot GPF(\theta,\phi)\cdot\tilde{j}(\theta,\phi)\cdot ISF(\theta,\phi)$$

where

$$C = 2\cdot 2j\cdot\frac{2}{k}\cdot C_k\,\eta\,I_o$$

$$AF(\theta,\phi) = \cos[\pi DP\sin\theta\sin\phi]$$

$$GPF(\theta,\phi) = \sin[2\pi H\cos\theta]$$

$$\tilde{j}(\theta,\phi) = \frac{\cos[\frac{\pi}{2}\sin\theta\sin\phi]}{[1-(\sin\theta\sin\phi)^2]}$$

$$ISF(\theta,\phi) = [\cos\theta\sin\phi\,\hat{\theta}+\cos\phi\,\hat{\phi}]$$

$$.....(3.11)$$

This total far-field function after normalizing can be written as sum of θ & φ components as:

$$G^n(\theta,\phi)=G^n_\theta(\theta,\phi)\hat{\theta}+G^n_\phi(\theta,\phi)\hat{\phi} \quad .....(3.12)$$

where

$$G^n_\theta(\theta,\phi)=AF(\theta,\phi)GPF(\theta,\phi)\tilde{j}(\theta,\phi)\cos\theta\sin\phi$$

$$G^n_\phi(\theta,\phi)=AF(\theta,\phi)GPF(\theta,\phi)\tilde{j}(\theta,\phi)\cos\phi$$

Further, since the dipoles are y-polarized, the copolar and crosspolar components of the far-field can be computed from eq. (3.12) by using copolar and crosspolar unit vectors in spherical coordinate system. Therefore,

$$G_{co}(\theta,\phi)=G^n_\theta(\theta,\phi)\cdot\sin\phi+G^n_\phi(\theta,\phi)\cdot\cos\phi \quad .....(3.13)$$

$$G_{xp}(\theta,\phi)=G^n_\theta(\theta,\phi)\cdot\cos\phi-G^n_\phi(\theta,\phi)\cdot\sin\phi \quad .....(3.14)$$

Eq. (3.12) gives the final expression for normalized far-field function of the two element broadside dipole array above infinite ground plane. It is clear from the equation that for half wavelength dipole the far-field function of the array depends only on separation between two dipoles (DP) and height of dipoles above ground plane (H). So it is possible to obtain the desirable pattern by carefully choosing the values of DP & H expressed in wavelengths.

3.2 Optimum values of DP & H to maximize aperture efficiency:

From the analysis in section 3.1, it is clear that for an array of two half wavelength dipoles on infinite ground plane, the radiation pattern depends only on distance between parallel dipoles (DP) & Height above ground plane (H). Imagine this pattern is used as a feed pattern for the reflector. The efficiency of the feed and reflector as a system, depends on the feed pattern and the half subtended angle of the reflector. So for given half subtended angle of the reflector, it is possible that we carefully choose the values of DP & H expressed in wavelengths, such that aperture efficiency is maximized.

To do this, DP & H values are varied within reasonable limits, and aperture efficiency for given half subtended angle of the reflector is evaluated for each possible combination of DP & H. Then maximum aperture efficiency is found out of these values and corresponding DP & H values are noted as the optimum values which maximize the aperture efficiency.

DP is varied from 0.42(λ) to 0.62(λ) in 0.01(λ) steps, while H is varied from 0.05(λ) to 0.5(λ) in 0.01(λ) steps. Thus aperture efficiency is computed for each possible combination of DP & H, giving total 966 combinations. And then maximum aperture efficiency is found from these values. Choice of the limits of DP & H is from the previous run of the program with higher variation of DP & H, but with coarser step. This whole analysis is repeated for various possible half subtended angles of the reflector ranging from 45° to 65° with 1° step. The results are summarized in Table 3.1 which shows the optimum values of DP & H expressed in wavelengths for each half subtended angle of the reflector and corresponding maximum aperture efficiency.

Table 3.1: Optimum values of DP & H

Θ_o^o	DPopt	Hopt	e_{ap}	e_{bor1}	e_{pol}	Peak Crosspol	BOR1 Crosspol
45	0.54	0.05	-1.166	-0.128	-0.001	-22.66	-36.08
46	0.52	0.05	-1.073	-0.112	0.000	-22.45	-42.15
47	0.51	0.05	-1.134	-0.105	0.000	-22.34	-41.82
48	0.49	0.05	-1.051	-0.092	0.000	-22.12	-37.34
49	0.48	0.08	-1.114	-0.088	0.000	-21.86	-35.31
50	0.48	0.18	-1.035	-0.096	0.000	-20.78	-33.90
51	0.48	0.21	-1.094	-0.100	0.000	-20.24	-33.22
52	0.48	0.25	-1.012	-0.107	-0.001	-19.31	-32.08
53	0.48	0.27	-1.066	-0.112	-0.001	-18.74	-31.40
54	0.48	0.30	-0.980	-0.120	-0.001	-17.72	-30.22
55	0.48	0.32	-1.031	-0.128	-0.001	-16.91	-29.29
56	0.48	0.34	-0.943	-0.136	-0.001	-15.97	-28.23
57	0.48	0.35	-0.990	-0.141	-0.001	-15.45	-27.64
58	0.48	0.37	-0.902	-0.153	-0.002	-14.47	-26.35
59	0.47	0.37	-0.947	-0.140	-0.004	-14.35	-24.89
60	0.47	0.39	-0.859	-0.152	-0.004	-13.45	-23.76
61	0.46	0.39	-0.903	-0.139	-0.007	-13.33	-22.55
62	0.45	0.40	-0.818	-0.133	-0.012	-12.78	-21.02
63	0.46	0.41	-0.862	-0.152	-0.010	-12.50	-21.59
64	0.45	0.42	-0.780	-0.145	-0.016	-11.99	-20.15
65	0.44	0.42	-0.825	-0.132	-0.022	-11.86	-19.28

3.3 Comparison with WiPl-D simulations:

From analytical pattern, the optimum values of DP & H are found to maximize aperture efficiency. From these values, it is possible to simulate the two element dipole array in WiPl-D software with infinite ground plane.

To compare the results obtained in Table 3.1 with WiPl-D simulations. The two element dipole array is simulated in WiPl-D for optimum DP & H values and then from simulated pattern feed efficiencies are computed.

Table 3.2 shows such comparison of feed efficiencies obtained from analytical pattern with simulated pattern from WiPl-D for half subtended angle of 50^o & 63^o.

Table 3.2: WiPl-D comparison

	$\theta_o=50^o$		$\theta_o=63^o$	
	Analytical	WiPl-D	Analytical	WiPl-D
e_{ap}	-1.035	-1.034	-0.862	-0.861
e_{BOR1}	-0.096	-0.094	-0.152	-0.151
e_{pol}	-0.0004	-0.0005	-0.0098	-0.0102
Peak XP	-20.78	-20.842	-12.50	-12.52
Peak BOR1 XP @ 45^o	-33.90	-33.83	-21.59	-21.56

For these two half subtended angles (50 & 63), corresponding copolar and crosspolar patterns in 45^o plane are plotted in Fig 3.4 & 3.7 respectively, and the 3D patterns are plotted in Fig. 3.5 & 3.8. Also the simulated patterns from WiPl-D are given for comparison in Fig 3.6 & 3.9.

Fig 3.4: Patterns for θ_o=50º

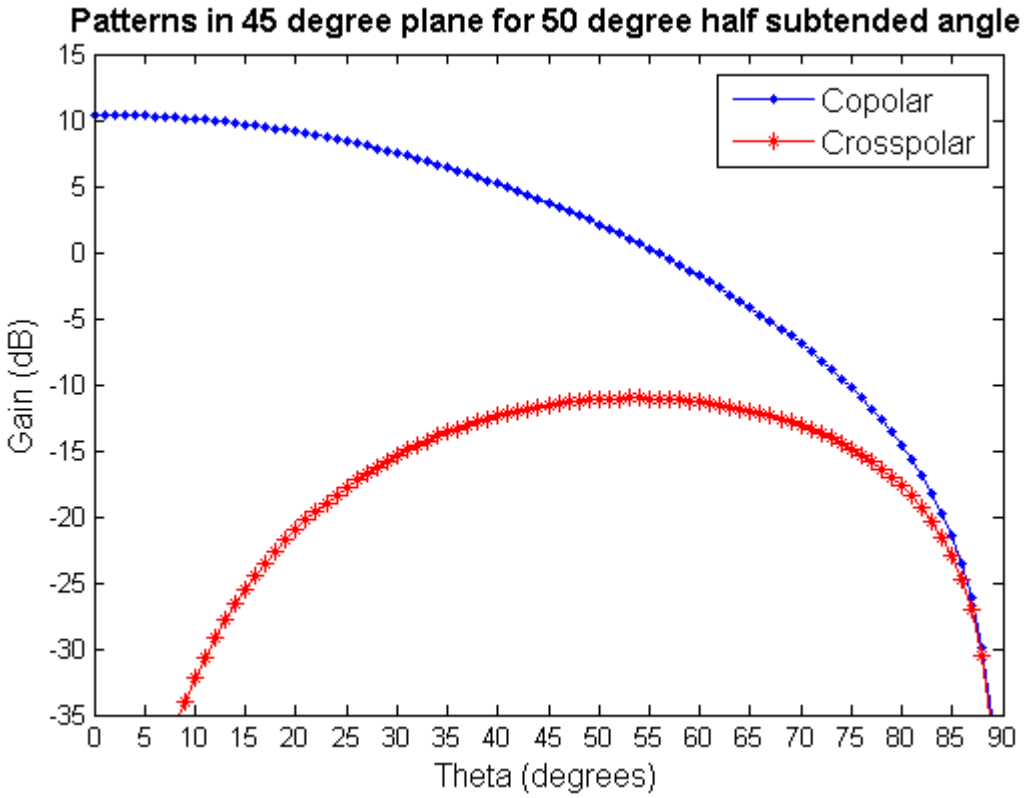

Fig 3.5: 3-D pattern for θ_o=50º (Linear Scale)

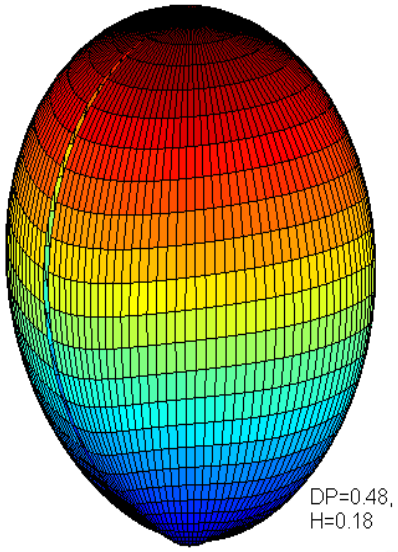

Fig 3.6: WiPl-D simulated pattern for θ_o=50º

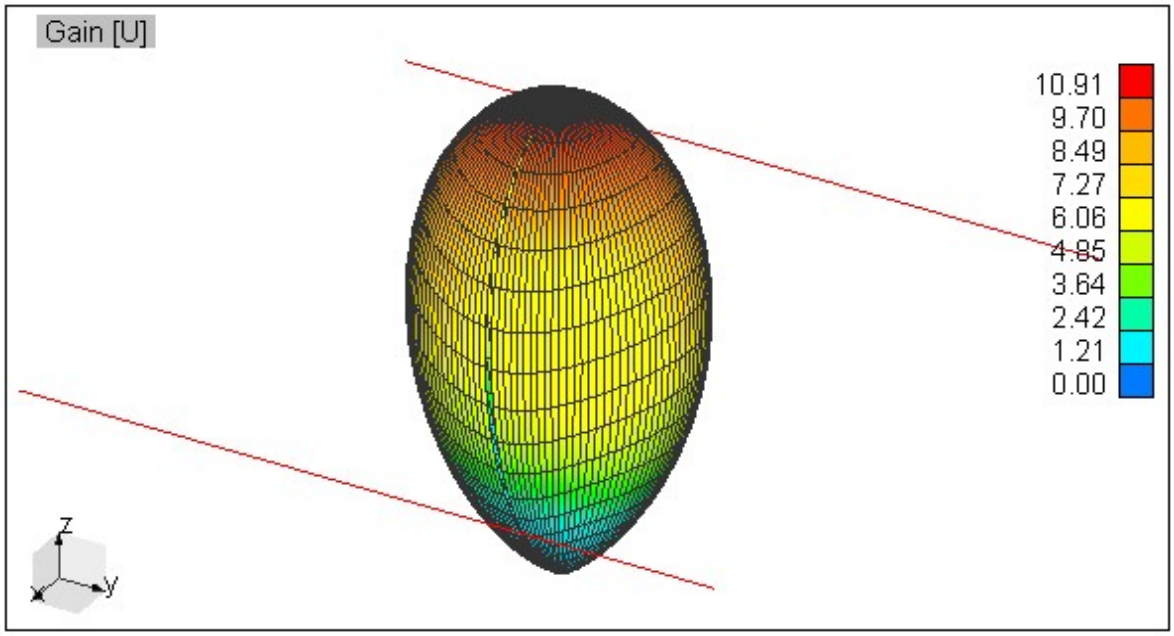

Fig 3.7: Patterns for θ_o=63º

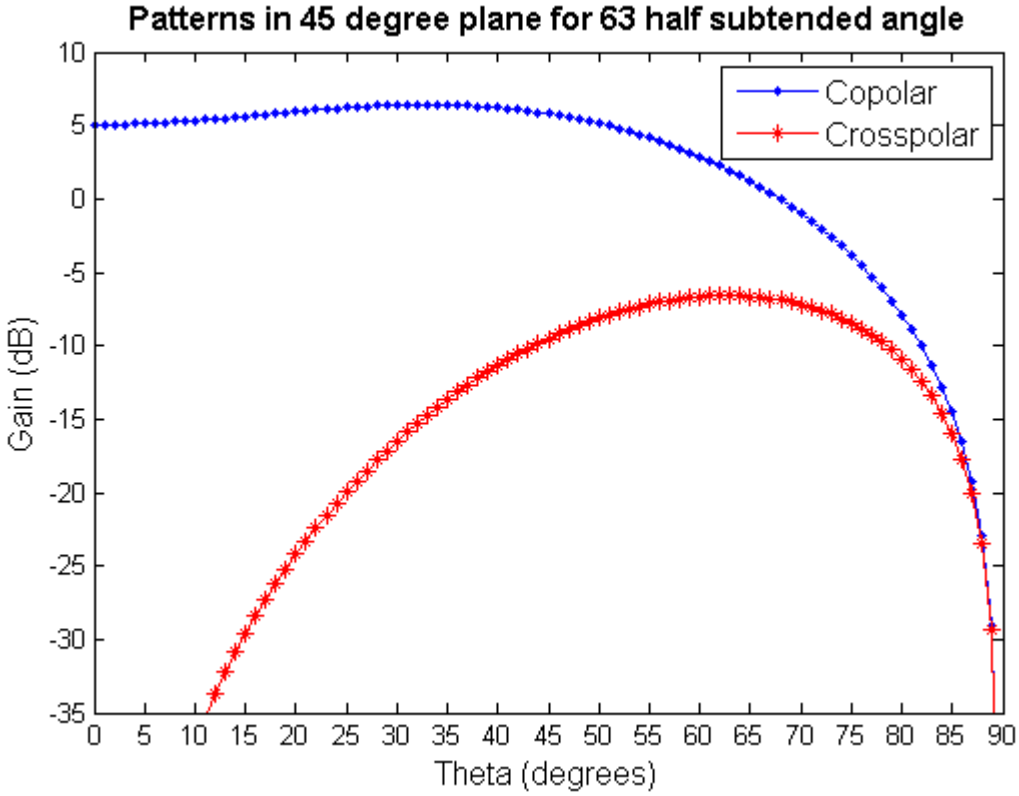

Fig 3.8: 3-D pattern for θ_o=63º
(Linear Scale)

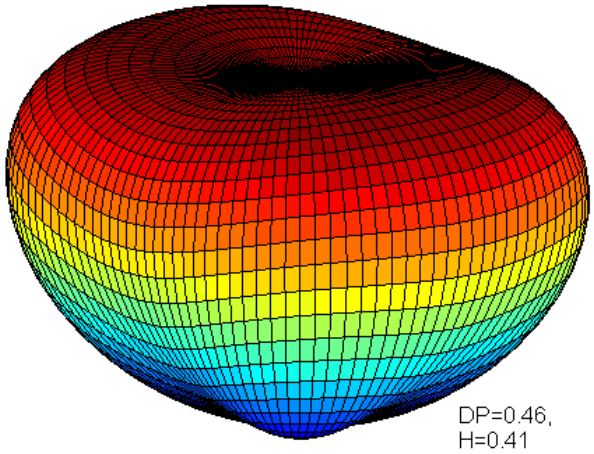

Fig 3.9: WiPl-D simulated pattern for θ_o=63º

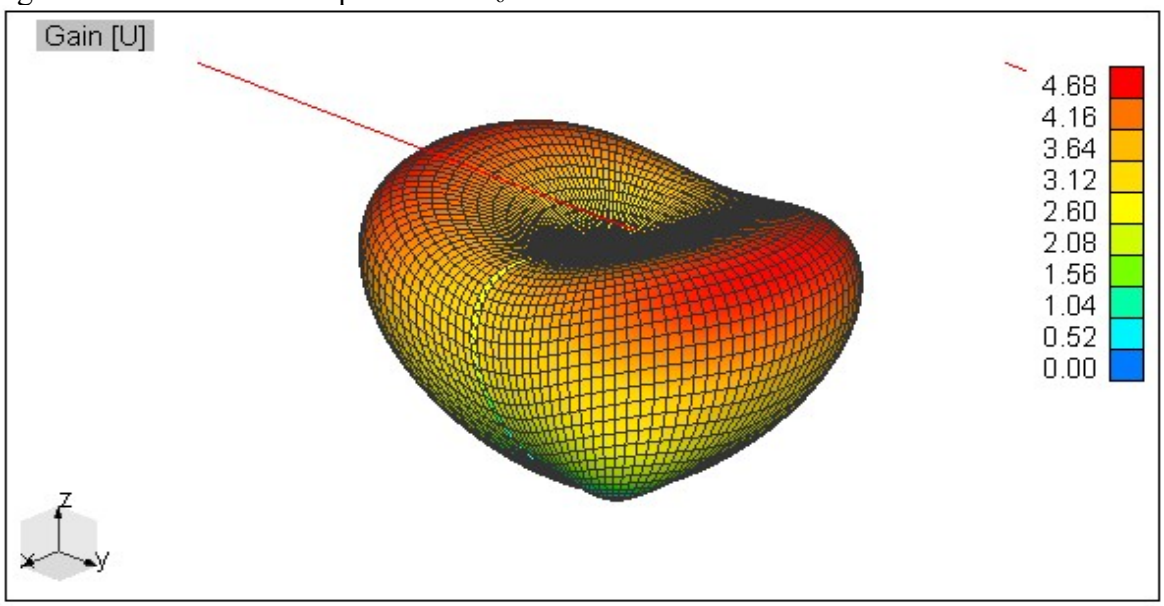

3.4 Effect of finite Ground plane:

Practically, the ground plane size is finite for the feed at the focus of the reflector. Finite ground causes the scattering at the edges, causing back lobes. This reduces the aperture efficiency, since the spill over increases. There exists a trade off on the size of finite ground plane; since the lowering the size increases spill over while making it larger causes more aperture blockage. Though in this analysis, the aperture blockage is not treated, the effect of finite ground plane on the aperture efficiency is studied in detail.

From the Table 3.1 we get the optimum values of DP & H over infinite ground plane for given half subtended angle of the reflector. Same values of DP & H are used to generate a computer model of the feed in WiPl-D software, and ground plane size is varied from 0.8(λ) to 2(λ) in 0.02(λ) steps. The simulated pattern from WiPl-D is then used to compute the aperture efficiencies for corresponding size of ground plane. Then ground plane size is chosen such that certain amount of degradation is accepted in the maximize aperture efficiency. (say 0.1dB). For GMRT the half subtended angle of the reflector is 62.5^o , so effect of finite ground plane is studied for 63^o half subtended angle of reflector. Fig 3.10 shows the effect of finite size ground plane on aperture efficiency. From this plot it is clear that as ground plane size increases the aperture efficiency reaches to ~ -1.0dB of maximum value with infinite ground plane. The choice of finite ground plane can be made such that one accepts certain amount of aperture efficiency say 70% (-1.55dB). Thus from fig 3.10 for 70% of aperture efficiency the ground plane size should be 1.64(λ) while for 60% aperture efficiency the size should be 0.88(λ).

The corresponding pattern of the feed with finite ground plane is also shown in Fig 3.11.

Fig 3.10: Effect of finite ground plane for θ_o=63^o

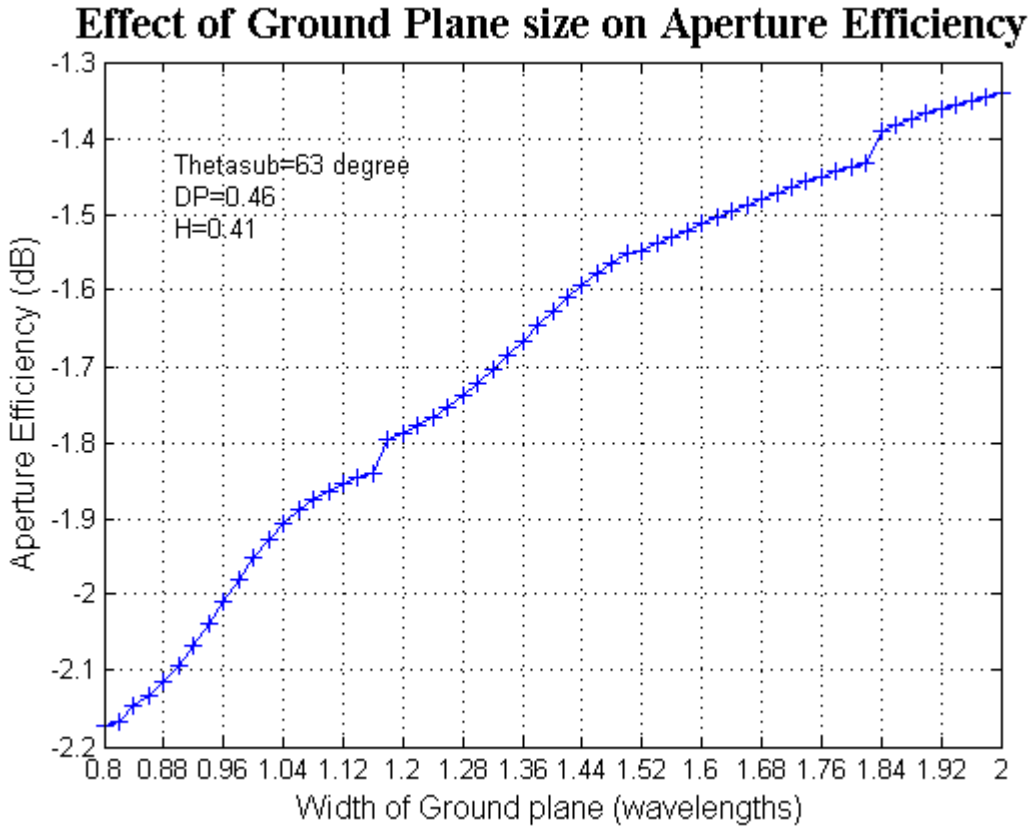

The corresponding pattern of the feed with finite ground plane is also shown in Fig 3.11.

Fig 3.11: Pattern with finite ground plane.

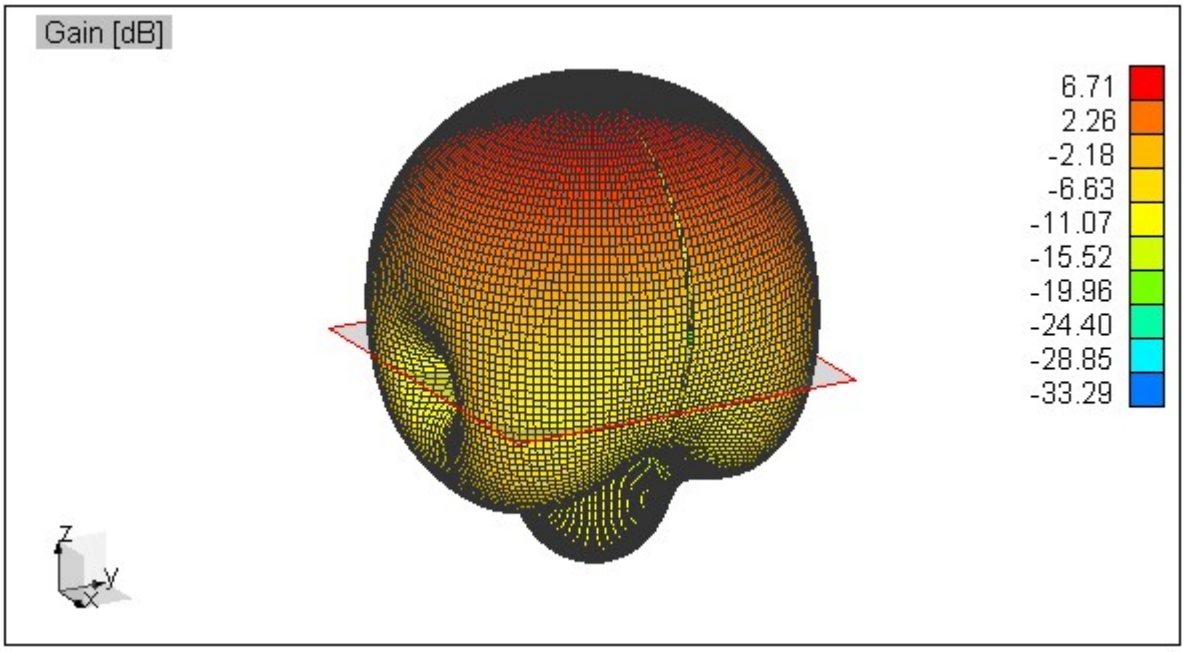

3.5 Conclusions:

1. For all half subtended angles the maximum aperture efficiency is ~ -1.0 dB (80%)
2. As θ_o increases the DP decreases while H increases.
3. Values given in Table 3.1, can be used to design the feed for the given θ_o.
4. Table 3.2 shows good agreement between the efficiencies values obtained analytically and from simulations.
5. The finite ground plane size can be then found from computer simulations.
6. For Eleven feed which is based on similar concept by replacing dipoles with folded dipoles, the above results can be useful.
7. The prior version of Eleven feed which uses DP=0.5 & H=0.16 with finite ground plane size of 0.88(λ), will work well for $\theta_o \sim 50^o$. Since for $\theta_o = 50^o$, DP=0.48 & H=0.18 which gives maximum aperture efficiency.

References:

[1] Kildal P.S., "Foundations of Antennas- A Unified Approach", Studentlitteratur, 2000.

4. Conventional Log Periodic Arrays of Dipoles

Making antennas broadband, is nothing but to make antenna performance independent of frequency. Theoretically, if the size of antenna and wavelength of operation is changed by same fraction, then the current distribution on the antenna remains fixed, this is the basic principle of frequency independent antennas.[1] Thus if any lossless system composed of mixture of dielectrics and metals which follows geometrical scaling principle will have its electrical performance independent of frequency when all of its dimensions are scaled in inverse proportion of frequency. i.e. Its dimensions measured in wavelengths are kept constant. It is also clear that if the shape of the antenna were such that it could be specified only by angles then its performance i.e. Pattern and impedance would be independent of frequency.[2]

To realize such antennas practically, planar & conical spirals had been tried which are convenient at centimeter wavelengths but becomes impractical at longer wavelengths. DuHamel & Isbell[3] first demonstrated another type of antenna whose shape was not solely described by angles, hence not truly frequency independent antenna but still having broadband behavior. This type of antenna is known as Log-periodic antenna because the impedance and pattern are periodic over a logarithm of frequency. DuHamel & Ore[4] further experimentally found log periodic antenna realized by thin wires instead of planar sheet structures. Finally Isbell[5] succeeded in developing a log periodic array of dipoles, in which he introduced an extra 180° phase shift from one dipole to next by switching the connections of transmission line feeding the dipoles. The through analysis of this type of antenna was then done by Carrel R.[6] in which he divided the problem into transmission line part and radiation part and analytically predicted the performance of log periodic dipole array of 8 elements with different scaling factors.

4.1 Log Periodic Dipole Array:

Conventional log periodic array of dipoles is formed by log periodically loading a transmission line by dipoles. The lengths of dipoles, radius of wire & the distance between them are scaled by a factor $\tau < 1$. The array is then fed at the shortest element i.e. The element corresponding to the highest geometrical frequency. The connection from one dipole to the next are switched so as to provide extra 180° phase shift as shown in fig 4.1

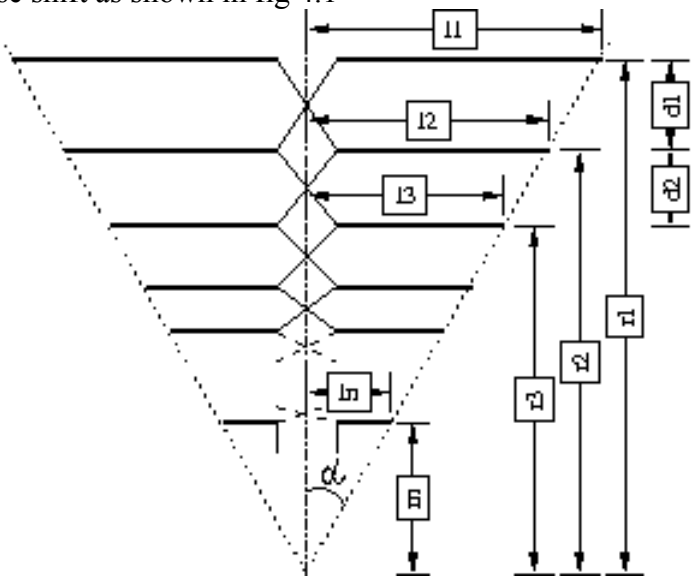

Fig 4.1: Log Periodic Array of Dipoles

The spacing 'dn' between one dipole to the next plays an important role in array operation. At particular value of 'dn' the phase delay in the transmission line combined with 180° phase shift due to switching the connections gives a total phase shift of $360°(1- dn/\lambda)$. This causes the radiated fields from two dipoles which are 'dn' apart in phase in backward direction. This results in good beam coming out of apex of the array giving endfire radiation.[2]

Theoretically this antenna to be frequency independent, all dimensions should be scaled in proportion to the distance from the origin. This also applies to the transmission line feeding the dipoles, so ideally it should be biconical. But if the spacing between the parallel wire line is

negligible as compared to the shortest wavelength of operation then the parallel wire line is equivalent to biconical line.[2] So practically we need not to scale the transmission line and hence the feed gap of all dipoles, if the spacing is small comparable to shortest wavelength ($s<<\lambda min$). Also in practical realizations the radius of wire forming the dipole is kept constant.

4.2 Geometrical Relations:

As seen from the Fig 4.1,

l_n = Length of n^{th} element

r_n = Distance from origin of n^{th} element

d_n = Spacing between the n^{th} and $(n+1)^{th}$ element

The entire geometry of array shown in Fig 4.1 can be written provided values of following parameters are know:

*f*min= Lowest Geometrical Frequency

N = Number of elements in an array

τ = Scaling factor (<1) which decides next geometrical freq.

σ = Spacing factor which decides the distance between consecutive dipoles. (λ)

l = Length of element (λ)

α = Opening angle of array

R = Radius of wire forming the dipole (λ)

From the principle of Log-periodic antennas, we know that all dimensions are scaled by a fixed scaling factor. So l_n, r_n, d_n are interrelated as follows:

$$\frac{l_{n+1}}{l_n}=\frac{r_{n+1}}{r_n}=\frac{d_{n+1}}{d_n}=\frac{R_{n+1}}{R_n}=\tau \qquad .....(4.1)$$

also r_n & d_n are interrelated as follows:

$$d_1=r_1-r_2$$

$$d_2=r_2-r_3$$

$$d_3=r_3-r_4$$

$$\text{Therefore}, d_n=r_n-r_{n+1}=r_n-\tau\cdot r_n$$

$$d_n=(1-\tau)\cdot r_n \qquad .....(4.2)$$

But d_n corresponds to spacing between consecutive dipoles which is a spacing factor when expressed in wavelengths. So,

$$\sigma=\frac{d_n}{\lambda_n}=(1-\tau)\cdot\frac{r_n}{\lambda_n} \qquad .....(4.3)$$

Now the opening angle of the array α can be expressed as follows:

$$\tan\alpha=\frac{l_1}{r_1}=\frac{l_n}{r_n}$$

by using eq. (4.1) & (4.3),

$$\tan\alpha=\frac{l\cdot\lambda_n}{\frac{\sigma\cdot\lambda_n}{(1-\tau)}}=\frac{l\cdot(1-\tau)}{\sigma}$$

$$\alpha=\tan^{-1}\left\{\frac{l\cdot(1-\tau)}{\sigma}\right\} \qquad .....(4.4)$$

If the dipoles are half wavelength long then the '*l*' is quarter wavelength. So by putting *l*=1/4 in the above formula, we get

$$\alpha=\tan^{-1}\left\{\frac{(1-\tau)}{4\sigma}\right\} \qquad .....(4.5)$$

which is same as that of eq (24) in paper by Carrel R.[6]

Apart from these parameters, the additional parameters are the spacing and diameter of the parallel wire transmission line feeding the array. Spacing and diameter values depends upon the system

characteristic impedance, with spacing $s<<\lambda$ such that parallel wire line tends to work as biconical one.

References:

[1] Rumsey V. H., "Frequency Independent Antennas", 1957 IRE National Convention Record, pt. 1, pp. 114-118.
[2] Rumsey V. H., "Frequency Independent Antennas", 1966 Academic Press.
[3] DuHamel R. H. & Isbell D. E., "Broadband Logarithmically Periodic Antenna Structures", 1957 IRE National Convention Record, pt. 1, pp. 119-128.
[4] DuHamel R. H. & Ore F. R., "Logarithmically Periodic Antenna Designs", 1958 IRE International Convention Record, pt.1, pp. 139-151.
[5] Isbell D. E., "Log Periodic Dipole Arrays", IRE Trans. Antennas & Propagation, vol. AP-8, pp.260-267, May 1960.
[6] Carrel R.L., "The Design of Log-Periodic Dipole Antennas", IRE Intern. Convention Record 1961, pt. 1, pp. 61-75.
[7] DuHamel R. H. & Berry D. G., "Logarithmically Periodic Antenna Arrays", IRE Wescon Conference Record 1958, pt. 1, vol. 2,pp. 161-174.
[8] Bell R. L., Elfving C. T. & Franks R. E., "Near-Field Measurements on a Logarithmically Periodic Antenna", IRE Trans. Antennas & Propagation,
vol. 8, Nov. 1960.
[9] Berry D. G. & Ore F. R., "Log Periodic Monopole Array", IRE International Convention Record, vol. 9, pt. 1, March 1961.
[10] Greiser J. W. & Mayes P., "The Bent Zigzag- A vertically Polarized Frequency Independent Antenna", IRE Trans. Antennas & Propagation, vol. 12, Issue 3, May 1964.
[11] Greiser J. W., "A new class of Log Periodic Antenna", IEEE Proceedings, vol. 52, Issue 5, May 1964.
[12] Balmain K. G. & Dyson J. D., "The Series Fed, Log Periodic Folded Dipole Array", International Symposium Antennas & Propagation Society, vol. 1, July 1963.
[13] Solosko R. & Laxpati S., "A Log Periodic Antenna with Vertically Polarized Omni directional Radiation", IRE Trans. Antennas & Propagation, vol. 16, issue 6, November 1968.
[14] Kyle R. H., "Mutual Coupling Between Log-Periodic Antennas", IRE Trans. Antennas & Propagation, vol. 18, issue 1, January 1970.
[15] Keen K., "A Planar Log-Periodic Antenna", IRE Trans. Antennas & Propagation, vol. 22, Issue 3, May 1974.
[16] Nurnberger et.al., "Analysis of the Log-Periodic Folded Slot Array", International Symposium Antennas & Propagation Society, vol. 2, June 1994.

5. Folded Dipole

Folded dipole antenna has become very common in use mainly because its easy to match with balanced line having higher characteristic impedance. Typically for half wave long folded dipole the input impedance is about 4 times to that of half wave dipole, while pattern is almost similar. Folded dipole has been successfully used before in Yagi's and also in Log-periodic antennas. In this chapter, the conventional folded dipole is described first and then through analysis of two port folded dipole is done which is a basic element of Folded Dipole Log Periodic Arrays.

5.1 Conventional Folded Dipole:

A conventional folded dipole is usually half wavelength long and is formed by the folding a wire to form a rectangular loop with spacing between the wires much smaller as compared to wavelength as shown in fig 5.1.

If the diameters of both parallel wires are same, then it is known as symmetric folded dipole else asymmetric since the current flowing through two wires will be unequal. Such type of folded dipoles can be analyzed by splitting the problem in transmission line part and antenna part as described by Uda & Mushiake[2].

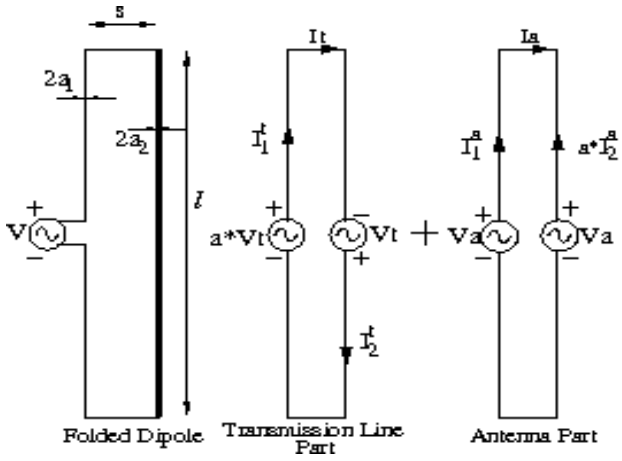

Fig 5.1: One Port Folded Dipole

Let,

V_t= Voltage for transmission line part

V_a= Voltage for antenna part

I^t= Current through loop in transmission line part

I^a= Current through loop in antenna part

V= Actual voltage applied at folded dipole terminals

a_1= radius of wire 1

a_2= radius of wire 2

s= Separation between two wires

I_1= Total current in wire 1 &

I_2= Total Current in wire 2.

Then the input impedance is ratio of V & I_1.

$$z_i = V / I_1 \quad \ldots(5.1)$$

$$I_1 = I_1^t + I_1^a \quad \ldots(5.2)$$

$$I_2 = I_2^t + I_2^a \quad \ldots(5.3)$$

$$I^t = I_1^t + I_2^t \quad \ldots(5.4)$$

$$I^a = I_1^a + I_2^a \quad \ldots(5.5)$$

The currents for antenna part in both wires are related to each other by current division factor defined by Uda & Mushiake[2] as:

$$I_1^a = a \cdot I_2^a \qquad .....(5.6)$$

where

$$a = \frac{\cosh^{-1}\frac{\nu^2-\mu^2+1}{2\nu}}{\cosh^{-1}\frac{\nu^2+\mu^2-1}{2\nu\mu}} \qquad .....(5.7)$$

$$\mu = \frac{a_2}{a_1} \ , \ \nu = \frac{s}{a_1} \qquad .....(5.8)$$

By making use of current division factor, the voltages V_t & V_a are related to V as:

$$a \cdot V_t + V_a = V$$

$$V_t - V_a = 0$$

This gives,

$$V_t = V_a = \frac{V}{1+a} \qquad .....(5.9)$$

5.1.1 Transmission Line Part:

This part can be seen as a parallel wire transmission line shorted at its ends, thus giving some impedance Z_t at its input. The equivalent circuit of the transmission line part is shown in fig 5.2.

By applying Kirchoff's laws,

$$a \cdot V_t + V_t = 2 \cdot Z_t \cdot I^t$$

$$I^t = \frac{(1+a)V_t}{2 \cdot Z_t} = \frac{V}{2 \cdot Z_t}$$

This gives,

$$I_1^t = -I_2^t = \frac{V}{2 \cdot Z_t} \qquad .....(5.10)$$

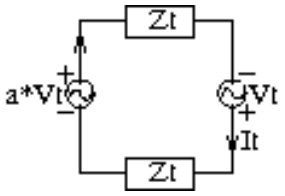

Fig 5.2: Equivalent Circuit

Here impedance Z_t depends upon the length of the dipole and the characteristic impedance of the parallel wire line formed by two wires and for lossless line, it is given by,

$$Z_t = j \cdot Z_c \tan\left(\frac{2\pi}{\lambda} \cdot \frac{l}{2}\right) \qquad .....(5.11)$$

The characteristic impedance of a parallel wire line formed by two wires with unequal radii based on current division factor is as follows[3][5]:

$$Z_c = 60 \cdot \left[\cosh^{-1}\frac{\nu^2-\mu^2+1}{2\nu} + \cosh^{-1}\frac{\nu^2+\mu^2-1}{2\nu\mu} \right] \qquad .....(5.12)$$

Apart from this, the accuracy of transmission line part can be improved if the extended length theory is used as suggested by Clark et.al.[6], in which author gives an empirical relation for the extended length of the transmission line as follows:

$$l_{extended} = l_{original} + \alpha s \qquad .....(5.13)$$

where the factor α is length extension factor and its value is empirical (α=0.39[6]). This extended length should also be used in antenna part while calculating the impedance of equivalent dipole.

5.1.2 Antenna Part:

Here the radiation coming out of two parallel wires is treated as the radiation from a single dipole having equivalent radius 'a_e', which is defined as[1][6]:

$$\ln a_e = \ln a_1 + \frac{1}{(1+\mu)^2}(\mu^2 \ln\mu + 2\mu \ln\nu) \qquad .....(5.14)$$

Let,

Z^a= Impedance of the dipole having equivalent radius a_e. Then,

$$Z_a = \frac{V_a}{I^a}$$

by using eq.(5.6),(5.9)

$$I^a = I_1^a + I_2^a = (1+a) I_1^a$$

$$I_1^a = \frac{I^a}{(1+a)} = \frac{V_a}{(1+a) Z_a}$$

This gives,

$$I_1^a = \frac{V}{(1+a)^2 Z_a} \qquad .....(5.15)$$

$$I_2^a = \frac{a \cdot V}{(1+a)^2 Z_a} \qquad .....(5.16)$$

5.1.3 Input Impedance:

From the analysis of transmission line and antenna part, we get the currents in both wires for these two modes. Thus the total current in both wires by using eq. (5.2) & (5.3) can be written as:

$$I_1 = V\left[\frac{1}{(1+a)^2 Z_a} + \frac{1}{2Z_t}\right] \qquad .....(5.17)$$

$$I_2 = V\left[\frac{a}{(1+a)^2 Z_a} - \frac{1}{2Z_t}\right] \qquad .....(5.18)$$

And finally the input impedance as defined in eq (5.1), can be written as inverse if input admittance:

$$Z_i = \frac{1}{Y_i}$$

where,

$$Y_i = \frac{I_1}{V}$$

$$Y_i = \frac{1}{(1+a)^2 Z_a} + \frac{1}{2Z_t} \qquad .....(5.19)$$

5.2: Two Port Asymmetric Folded Dipole:

The conventional folded dipole can be thought of as a two port as if its second port is short circuits. So two port folded dipole can be formed by breaking the rectangular loop along the feeder line of conventional folded dipole. This type of folded dipole is then useful in log periodic arrays where several two port folded dipoles are cascaded log periodically. For analysis of such two port folded dipole author proposes the use of superposition theorem. Since the two port folded dipole can be thought of as, a superposition of two conventional folded dipoles with either ports short circuited as shown in fig 5.3.

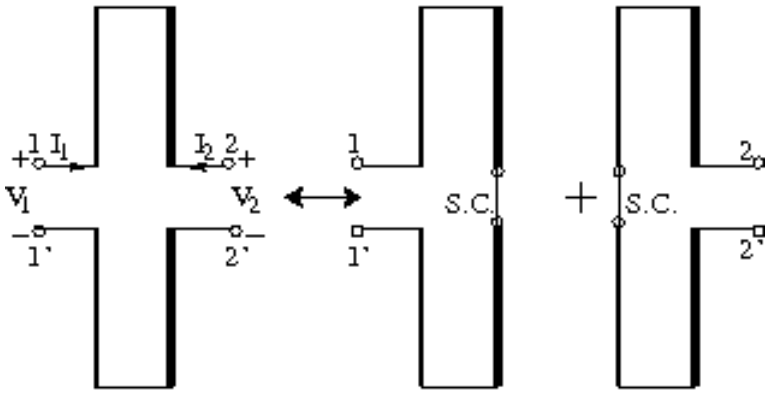

Fig 5.3: Two Port Folded Dipole

When Port 2 is short circuited, the currents in both dipole wires can be written by using eq. (5.17) & (5.18) as:

$$I_1' = V_1\left[\frac{1}{(1+a)^2 Z_a} + \frac{1}{2Z_t}\right] \quad .....(5.20)$$

$$I_2' = V_1\left[\frac{a}{(1+a)^2 Z_a} - \frac{1}{2Z_t}\right] \quad .....(5.21)$$

Similarly when port 1 is short circuited, the currents in both wires are written as:

$$I_1'' = V_2\left[\frac{a'}{(1+a')^2 Z_a} - \frac{1}{2Z_t}\right] \quad .....(5.22)$$

$$I_2'' = V_2\left[\frac{1}{(1+a')^2 Z_a} + \frac{1}{2Z_t}\right] \quad .....(5.23)$$

where new current division factor a' is introduced since when fed from port 2 the radii of two conductors are interchanged. So definition of a' is same as given in eq. (5.7) except,

$$\mu = \frac{a_1}{a_2} \quad , \quad \nu = \frac{s}{a_2} \quad .....(5.24)$$

Now by using superposition theorem, we can write the total current I_1 & I_2 as follows:

$$I_1 = \left[\frac{1}{(1+a)^2 Z_a} + \frac{1}{2Z_t}\right]V_1 + \left[\frac{a'}{(1+a')^2 Z_a} - \frac{1}{2Z_t}\right]V_2 \quad .....(5.25)$$

$$I_2 = \left[\frac{a}{(1+a)^2 Z_a} - \frac{1}{2Z_t}\right]V_1 + \left[\frac{1}{(1+a')^2 Z_a} + \frac{1}{2Z_t}\right]V_2 \quad .....(5.26)$$

eq.(5.25), (5.26) are of the form of admittance matrix of two port network,

$$\begin{bmatrix} I_1 \\ I_2 \end{bmatrix} = \begin{bmatrix} Y_{11} & Y_{12} \\ Y_{21} & Y_{22} \end{bmatrix}\begin{bmatrix} V_1 \\ V_2 \end{bmatrix}$$

where

$$Y_{11} = \left[\frac{1}{(1+a)^2 Z_a} + \frac{1}{2Z_t}\right] \quad .....(5.27)$$

$$Y_{12} = \left[\frac{a'}{(1+a')^2 Z_a} - \frac{1}{2Z_t}\right] \quad .....(5.28)$$

$$Y_{21} = \left[\frac{a}{(1+a)^2 Z_a} - \frac{1}{2Z_t}\right] \quad .....(5.29)$$

$$Y_{22} = \left[\frac{1}{(1+a')^2 Z_a} + \frac{1}{2Z_t}\right] \quad .....(5.30)$$

Further it can be proved that a'= 1/a, hence substituting value of a' in eq. (5.28) & (5.30),

$$Y_{12} = \left[\frac{a}{(1+a)^2 Z_a} - \frac{1}{2Z_t}\right] \quad .....(5.31)$$

$$Y_{22} = \left[\frac{a^2}{(1+a)^2 Z_a} + \frac{1}{2Z_t}\right] \quad .....(5.32)$$

Thus $Y_{12}=Y_{21}$, indicates reciprocal two port network with its equivalent π network as shown in fig 5.4.

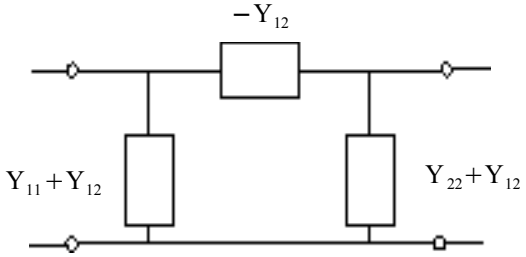

Fig 5.4: Equivalent π Network of Two Port Folded Dipole

5.3 Condition for equal Input & Load Impedance:

Once the admittance matrix of two port folded dipole is known, it is possible to derive the condition to have same input impedance at port 1 as that of load impedance at port 2. i.e. $Z_i=Z_L$. For any two port lossless network, the input admittance is given by,

$$Y_i = Y_{11} - \frac{Y_{12}^2}{Y_L + Y_{22}} \qquad .....(5.33)$$

but $Y_i = Y_L$

$$Y_L = Y_{11} - \frac{Y_{12}^2}{Y_L + Y_{22}}$$

Further if the dipole is symmetric, then $a = 1$ giving $Y_{11} = Y_{22}$

Thus,

$$Y_L^2 = Y_{11}^2 - Y_{12}^2$$

$$Y_L = \sqrt{Y_{11}^2 - Y_{12}^2} \qquad .....(5.34)$$

By using eq.(5.27), (5.28)

$$Y_L = \sqrt{\frac{1}{2Z_a Z_t}} \qquad .....(5.35)$$

$$Z_L = \sqrt{2Z_a Z_t} \qquad .....(5.36)$$

Thus eq. (5.36) gives the condition which when satisfied will give same input impedance at port 1 as that of load impedance at port 2.

5.4 Results & Comparisons:

In section 5.2, the admittance matrix of two port folded dipole is derived, so it is possible to predict the input impedance of two port folded dipole for given load impedance provided the input impedance of equivalent dipole is known which can be found by method of moments.

Here, the two port folded dipole is first simulated in WiPl-D software and then results are compared to the analytically ones by making use of equivalent dipole impedance simulated by WiPl-D. Variety of cases has been tried with different wire diameters, spacing, lengths & loads. Figures below shows the comparison of impedances calculated from simulations and theory described in sec. 5.2. Figure 5.5 shows the conventional symmetric folded dipole while fig. 5.6 & 5.7 shows the asymmetric with different loads at port 2.

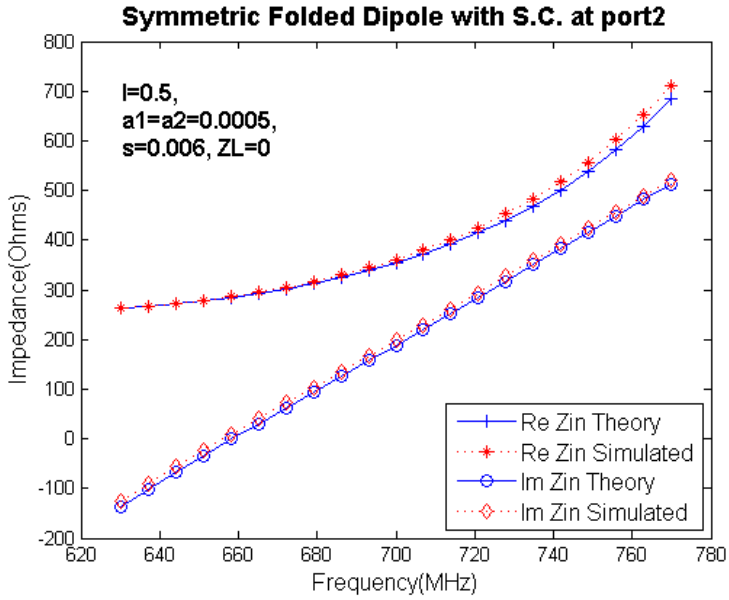

Fig 5.5: Symmetric Folded Dipole

One can observe that good agreement between theory & simulations by Method of moments is achieved for all cases presented here. Fig 5.8 shows folded dipole with comparatively large spacing between two parallel wires, and then it is observed that theoretical values deviate from simulated ones.

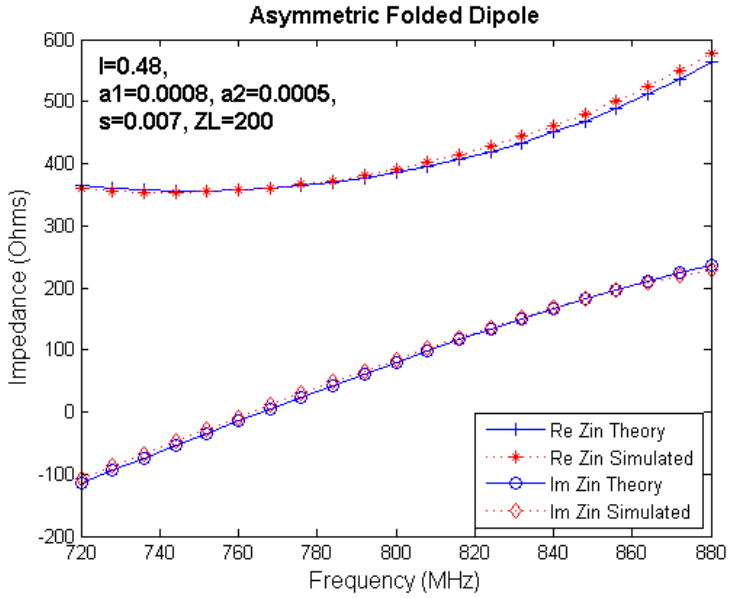

Fig 5.6: Asymmetric Folded Dipole with Resistive Load

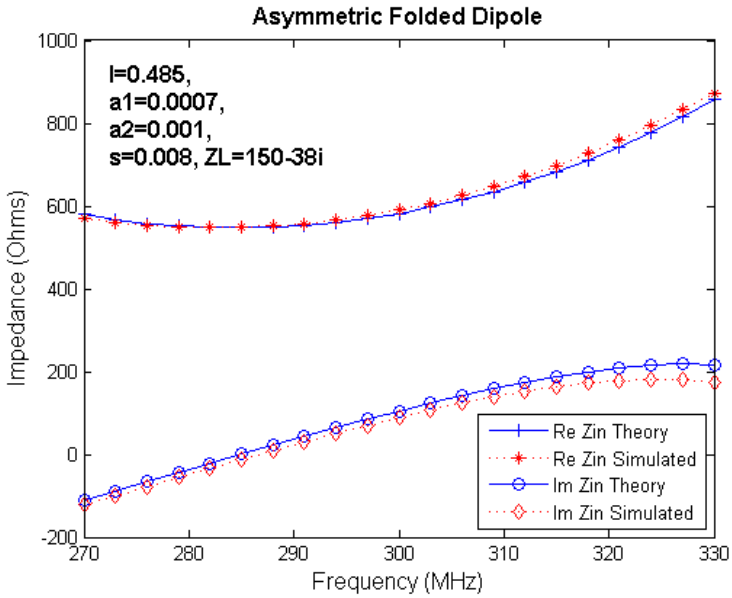

Fig 5.7: Asymmetric Folded Dipole with Complex Load

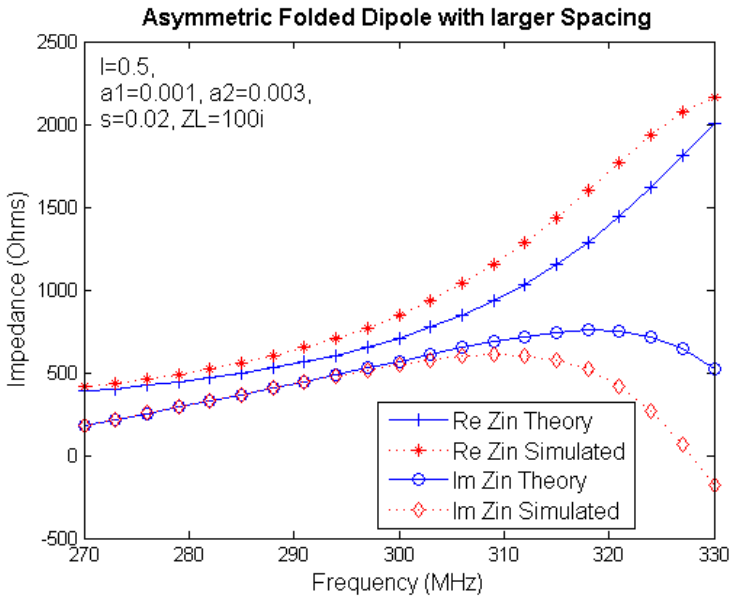

Fig 5.8: Effect of larger spacing

5.5 Conclusions:

Theory described in section 5.2, shows good agreement with the simulated input impedance from method of moments for thin wires (a1, a2 << λ). This shows the superposition principle works well for two port folded dipole. As seen from fig 5.8, the accuracy of this model depends upon the spacing between the two parallel wires so that the usual transmission line formulas are applicable. The maximum spacing of 's<0.01λ' seems reasonable.[4]

References:

[1] Jasik & Johanson, "Antenna Engineering Handbook", 2nd edition, McGraw-Hill 1984.

[2] S. Uda & Y. Mushiake, "Yagi-Uda Antenna", Tokyo, Japan: Maruzen, 1954.

[3] German J. P. & Brooks F. E., "The Effects of the Physical Parameters on the Bandwidth of a Folded Dipole", IRE Trans. Antennas & Propagation, April 1958.

[4] Thiele et. al., "On the Accuracy of the Transmission Line Model of the Folded Dipole", IEEE Trans. Antennas & Propagation, vol. AP-28, No. 5, September 1980.

[5] Chen-To Tai, "Theory of Terminated Monopole", IEEE Trans. Antennas & Propagation, vol. AP-32, No. 4, April 1984.

[6] Clark A.R., Fourie A. P. C., "An Improvement to the Transmission Line Model of Folded Dipole", IEEE Proceedings-H, vol. 138, No. 6, December 1991.

[7] Shintkin et.al., "Analysis of Log-Periodic Folded Dipole Array", IEEE 1992.

6. Folded Dipole Log-Periodic Arrays in Free Space

In conventional dipole log-periodic arrays, switching is required in consecutive dipole elements for proper phasing, this disadvantage is overcome by making use of folded dipoles in log periodic arrays. The half wavelength long folded dipole gives approximately 180^o phase difference from port1 to port2, which avoids switching. Also the higher input impedance of folded dipole helps to match array to higher characteristic impedance of parallel wire line.

6.1 Optimization Parameters:

The entire geometry of Folded Dipole Log-Periodic array (FDLPA) of wires can be written with knowledge given in table 6.1 & corresponding array is shown in fig 6.1.

Table 6.1: Optimization Parameters

f_{min}= Lowest Geometrical Frequency
N = Number of elements in an array
τ = Scaling factor (<1) which decides next geometrical freq.
σ = Spacing factor which decides the distance between consecutive dipoles. (λ)
l = Length of element (λ)
a1 = Radius of wire at port 1 of folded dipole (λ)
a2 = Radius of wire at port 2of folded dipole (λ)
s = Spacing between two wires (λ)
K1 = Low Frequency Truncation Constant
K2 = High Frequency Truncation Constant

Out of these optimization parameters the first 5 parameters are same as that of dipole LPA as discussed in chap 4 and relation between them is given by eq. (4.1), (4.3) & (4.4). Parameters a1, a2 & s decides the dimensions of the individual folded dipole, while parameters K1 & K2 are optional but useful of better impedance matching of the array. K1 & K2 are numerical constants and are known as truncation constants, since they alter the length of first (low freq.) & last element (high freq) in order to reduce the impedance variations. Ideally the array should be of infinite elements, but in practice the log periodic array is of finite number of elements and hence to reduce this effect of truncation, K1 & K2 are introduced as truncation constants.

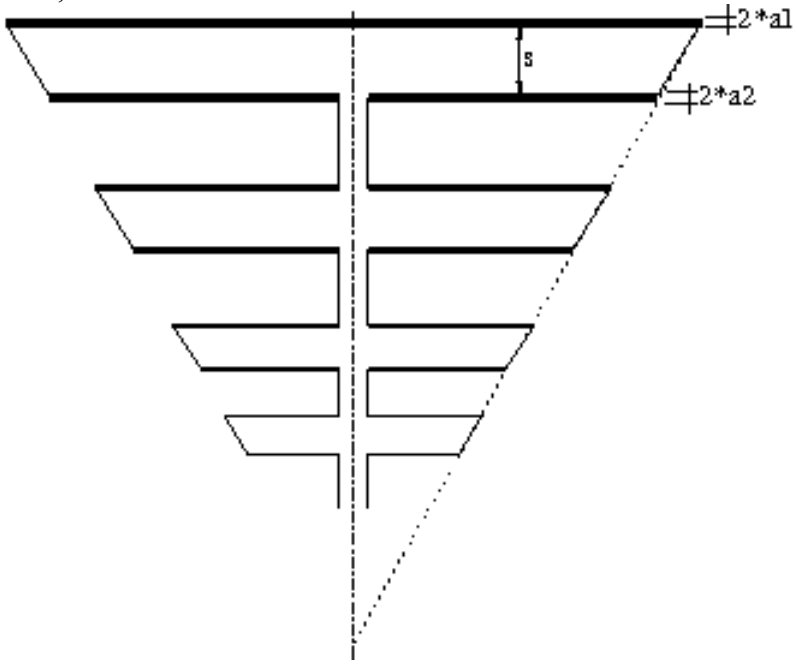

Fig 6.1: Folded Dipole Log-Periodic Array

First the entire geometry of the array is written with knowledge of f_{min}, N, τ, σ & *l*. Then truncation constants are used to alter the lengths of first & last element as follows:

$$l_1^{altered} = K1 \cdot l_1^{original} \quad .....(6.1)$$

$$l_n^{altered} = K2 \cdot l_n^{original} \quad .....(6.2)$$

Apart from these parameters, additional parameters required are feedgap & radius of wire feeding the dipoles. Feedgap basically decides the separation between two parallel wire lines, and hence decides the characteristic impedance of parallel wire line feeding all the folded dipoles provided it is kept constant through out the array. If feedgap is much smaller as compared to shortest wavelength of operation we need not to scale the transmission line. (feedgap << λ_{min}). If feedgap is assumed then the radius of wire feeding the dipoles can be computed with the knowledge of required characteristic impedance of parallel wire line by using following formula.

$$R_{feedwire} = \frac{feedgap}{2 \cdot \cosh \frac{Z_o}{120}} \quad .....(6.3)$$

6.2 Example of Wire FDLPA:

Fig 6.2 shows the geometry of wire FDLPA in WiPl-D software. The antisymmetry plane is used, so that modeling of only half structure of the array is required. The array is fed at the shortest element. The antisymmetry plane causes odd mode to exists in the structure which results in proper beam coming out of the apex of the array as shown in fig 6.3.

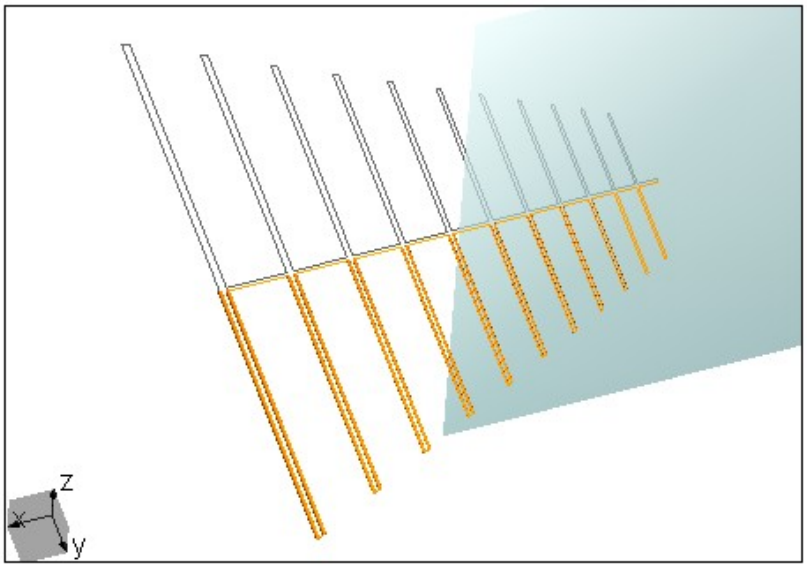

Fig 6.2: FDLPA Geometry in WiPl-D

The above FDLPA is designed with following parameters:
f_{min}=200MHz, N=11, τ=0.885, σ=0.0542, l=0.47, a1=a2=0.0017, s=0.006.

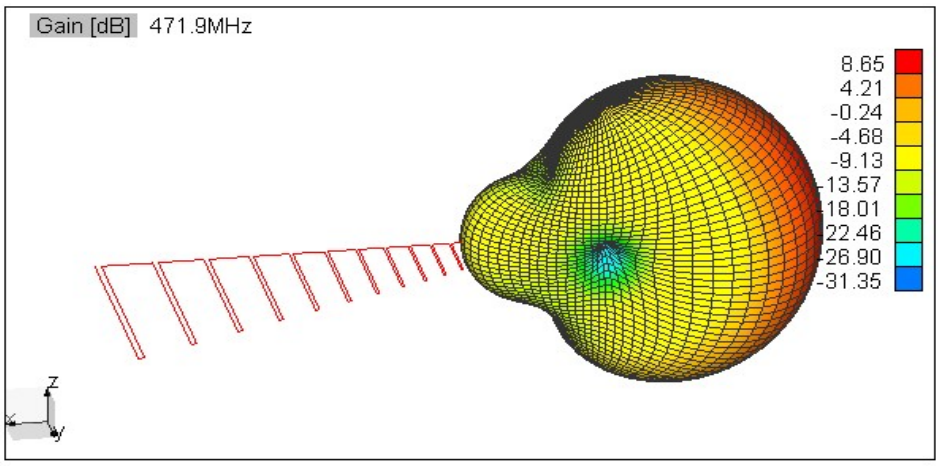

Fig 6.3: FDLPA Radiation

For this array, the magnitude of input reflection coefficient for 300Ω characteristic impedance is shown in fig 6.4. The geometrical lower & higher cutoff of the array is 200MHz & 678.5MHz respectively. It seen that S11 is less than -10dB over large part of the band. (~231MHz to 515MHz). This band is usually called the active region of the array in which the impedance & pattern has less variations.

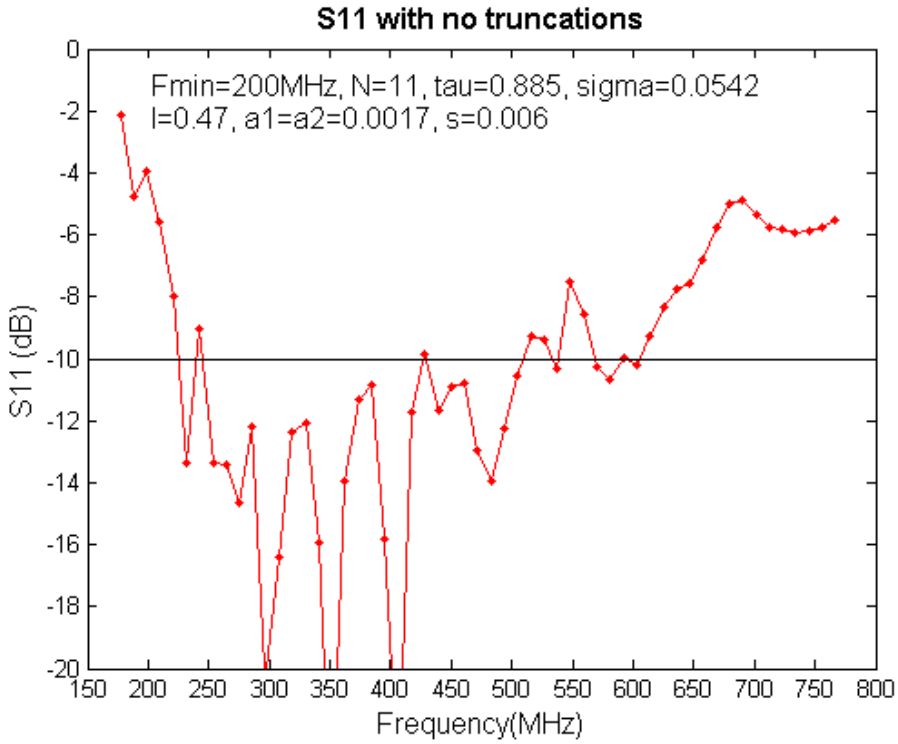

Fig 6.4 S11vs Frequency

The next thing to understand is the effect of truncation constants. Low & High frequency truncation constants has a strong effect on S11 at lower & higher frequencies respectively. This effect is shown in fig 6.5, while fig 6.6 shows the S11 when both truncations are used.

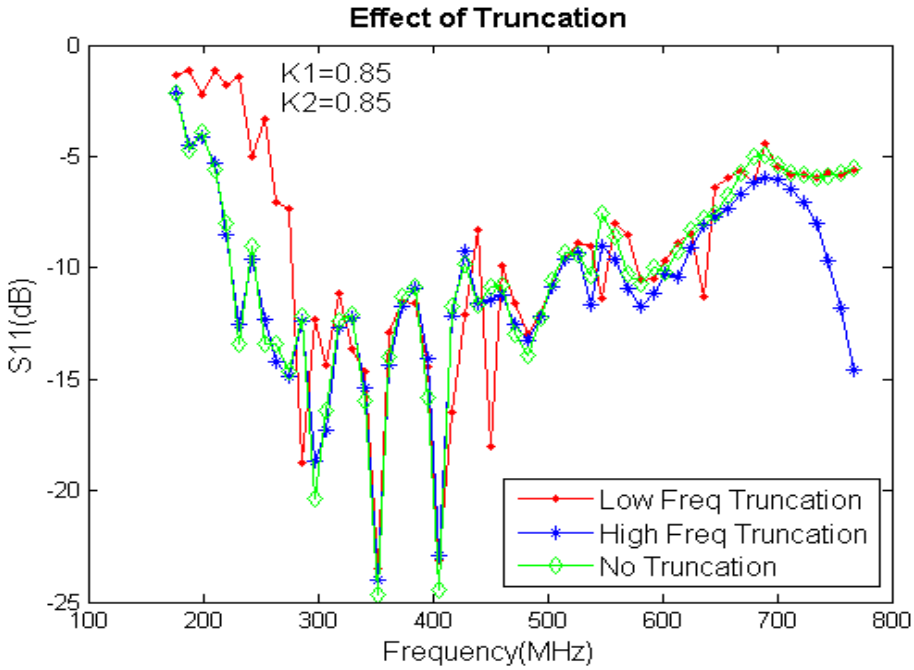

Fig 6.5: Effect of Truncation on S11

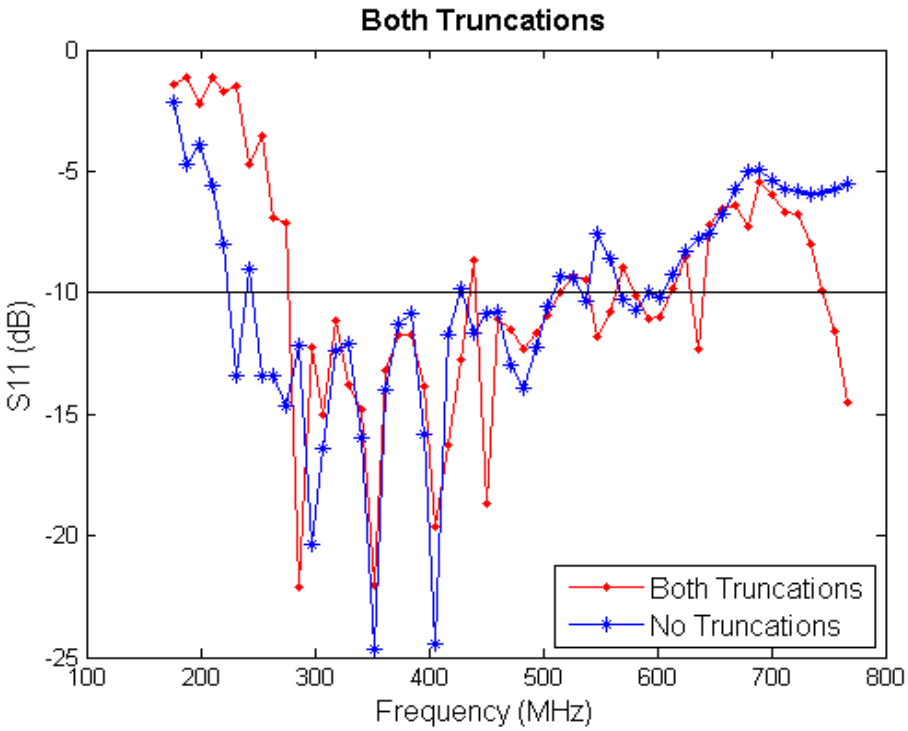

Fig 6.6: Use of Both Truncations

6.3 Conclusion:

1. Complete geometry of the array can be written with only use of optimization parameters.
2. The choice of these parameter values is empirical and needs to be optimize for better impedance matching.
3. Spacing constant (σ) plays an important role in matching, since it decides the phasing from one element to next.
4. Truncation constants K1 & K2 has effect on S11 on lower & higher frequencies of the band respectively.
5. Though K1 & K2 are optional, better impedance matching can be achieved by careful choice of K1 & K2.
6. Constant width transmission line can be used to feed all folded dipoles. i.e. Scaling of transmission line is not required.

7. Stripe Line Studies

For wire FDLPA discussed in chap.6, the constant width parallel wire line is used to feed the array. Similarly for FDLPA formed of metal plates instead of wires, parallel plate line is required to feed them.

The characteristic impedance of such parallel wire line can be predicted analytically if zero thickness is assumed[1] which depends upon the separation 's' between two parallel plates & width 'w' of the plate and is given as:

$$Z_o = 120 \cdot \pi \cdot \frac{K(k)}{K(k_1)} \qquad .....(7.1)$$

where,

$$k = \frac{s}{(s+2 \cdot w)}$$

$$k_1 = 1 - k^2$$

$K(k), K(k_1)$ are complete elliptic integrals of first kind.

The effect of finite thickness though discussed in various literature[2][3][4][5], simulations in WiPl-D are used to design a proper parallel plate transmission line for 200Ω of characteristic impedance. Fig 7.1 shows the geometry of such line, while fig 7.2 shows the return loss of the line when terminated with 200Ω impedance.

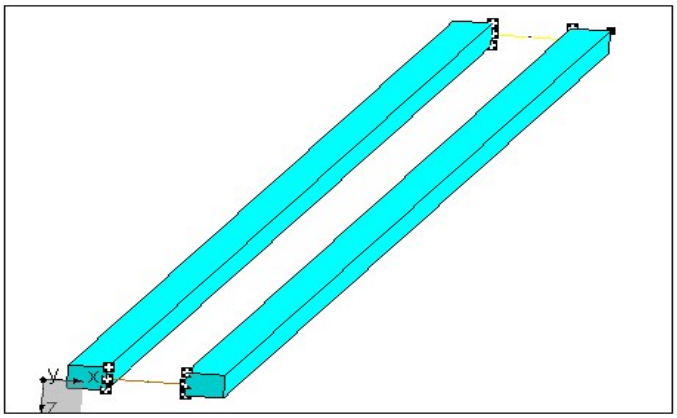

Fig 7.1: WiPl-D model of Parallel Plate Line

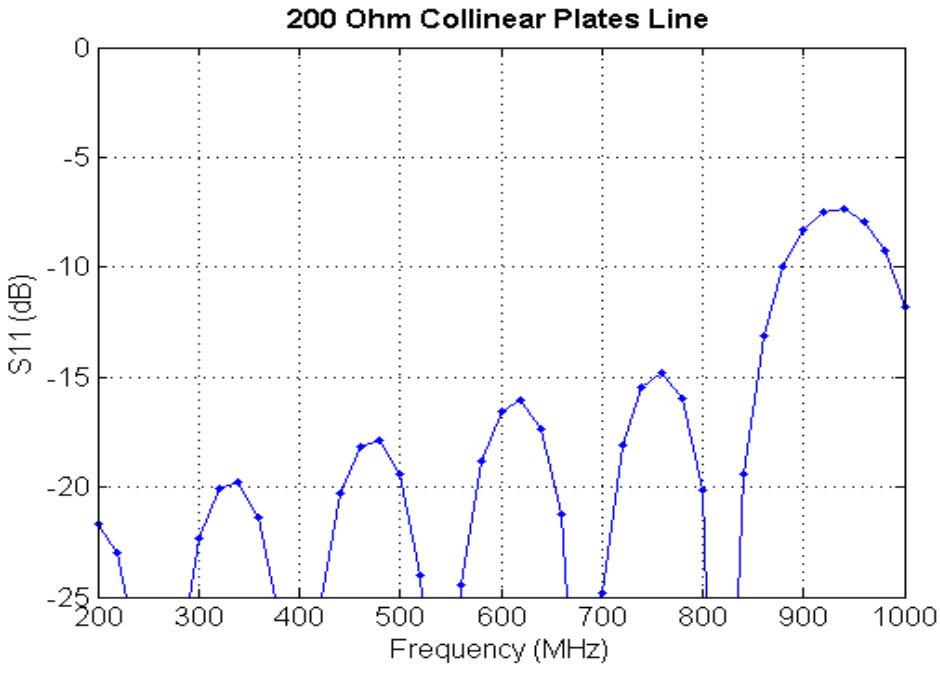

Fig 7.2: S11 for Parallel Plate Line

From simulations the best geometrical values of parallel plate line for 200Ω of characteristic impedance are as follows:

s = 6 mm
w = 3 mm
t = 2 mm

It is seen from S11 plot that the line has characteristic impedance of approximately 200Ω for 200-800MHz band, so this line will be used to feed plate FDLPA.

References:

[1] Jasik & Johanson, "Antenna Engineering Handbook", 2nd edition, McGraw-Hill 1984.
[2] Park D., "Planar Transmission Lines", IRE Trans. Microwave Theory & Techniques, April 1955.
[3] Cohn S., "Characteristic Impedance of Broadside-Coupled Stripe Transmission Lines", IRE Trans. Microwave Theory & Techniques, November 1960.
[4]Cohn S., "Thickness Corrections for Capacitive Obstacles & Stripe Conductors", IRE Trans. Microwave Theory & Techniques, November 1960.
[5] Yang et.al.,"Analysis of Characteristic Impedance of Stripe Double Line", IEEE Symposium Microwave, Antenna, Propagation, 2005.

8. Plate FDLPA

Folded Dipole Log Periodic Array of metal plates is very similar to wire FDLPA discussed in chap. 6, with only difference of wires being replaced by metal plates. For manufacturing reasons, the thickness of metal plate is constant throughout the array which is a limitation since thickness should also get scaled log periodically. This limitation is overcome by properly choosing the widths of metal plates.

Optimization parameters of plate FDLPA are also similar to wire FDLPA, except a1,a2 & s are now replaced with w1, w2 & g respectively, where w1 & w2 represents the width of plate at port 1 & port 2 respectively and g represents the gap between the parallel plates, all expressed in wavelengths. To model such array in WiPl-D the basic folded dipole is modeled with some finite thickness, which is achieved by making metal box of infinitesimally thin metal plates. And then other folded dipoles in array are just scaled replicas of the first one. Also antisymmetry plane is used so that modeling of only half structure is required. Fig 8.1 shows such folded dipole formed by joining infinitesimally thin metal plates, and table 8.1 defines the coordinate of it.

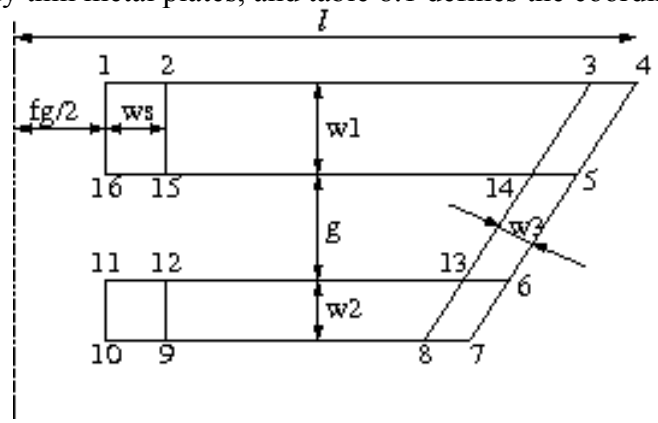

Fig 8.1: Folded Dipole of Metal Plates

Table 8.1: Node Coordinates

Node No.	X-Coordinate	Y-Coordinate
1	r	fg/2
2	r	fg/2+ws
3	r	*l*- w3/cos(α)
4	r	*l*
5	r-w1	*l*- w1*tan(α)
6	r-w1-g	*l*- (w1+g)*tan(α)
7	r-w1-g-w2	*l*- (w1+g+w2)*tan(α)
8	r-w1-g-w2	*l*- (w1+g+w2)*tan(α)- w3/cos(α)
9	r-w1-g-w2	fg/2+ws
10	r-w1-g-w2	fg/2
11	r-w1-g	fg/2
12	r-w1-g	fg/2+ws
13	r-w1-g	l- (w1+g)*tan(α)- w3/cos(α)
14	r-w1	*l*- w1*tan(α)- w3/cos(α)
15	r-w1	fg/2+ws
16	r-w1	fg/2

Where

fg= Feed gap for all folded dipoles

ws= width of stripe of parallel plate line.

α= Opening angle of the array as defined in eq. (4.4)

r= distance of element from array origin.

Note- fg & ws comes from stripe line studies

For next folded dipole in an array, all the dimensions get scale by scaling factor (τ), except the feed gap and width of stripe feeding the folded dipole. Fig 8.2 shows the complete Wipl-D geometry of such array and fig 8.3 shows corresponding return loss of the array designed for 200Ω of characteristic impedance. The shorting stub is used on longest element to have better impedance matching. The optimization parameters of this plate-FDLPA are as follows:
f_{min}=170MHz, N=16, τ=0.89, σ=0.0467, *l*=0.46, w1=w2=0.013, g=0.0065, K1=K2=0.85, Short=0.025(λ_{max})
fg=6mm & ws=3mm, thickness of metal plate=2mm.

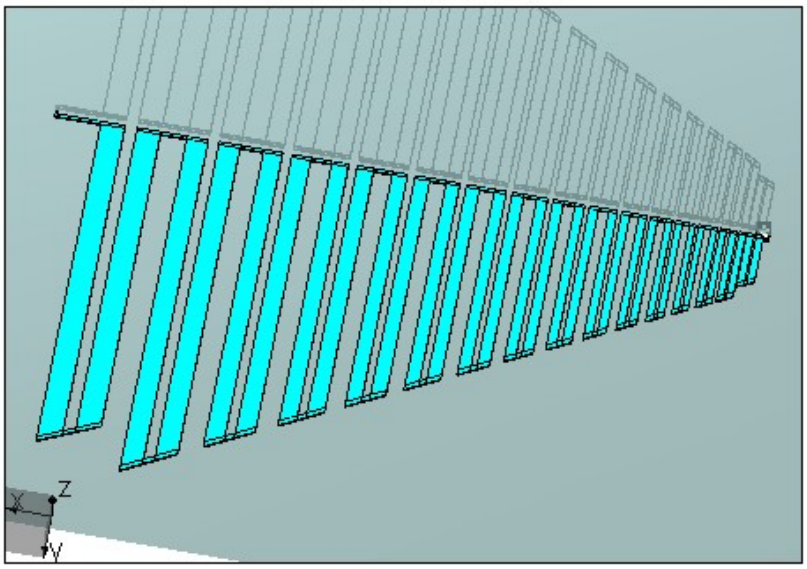

Fig 8.2: WiPl-D model of Plate-FDLPA

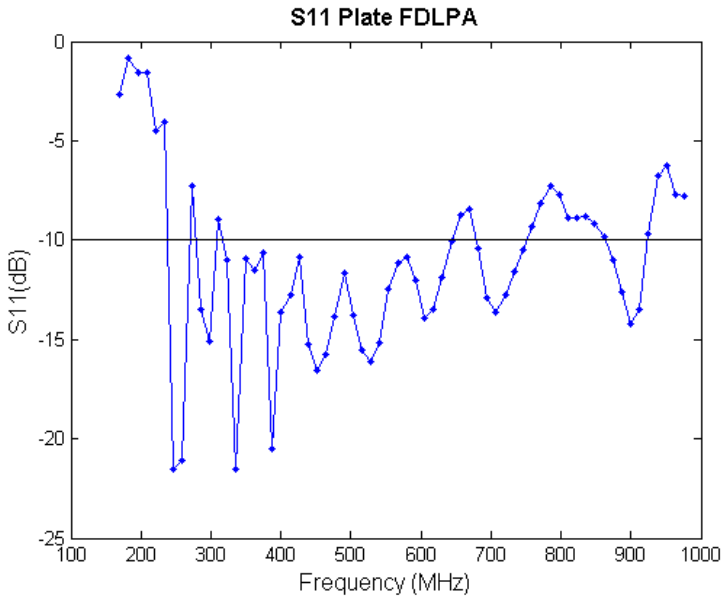

Fig 8.3: S11 of Plate-FDLPA for Z_o=200Ω

Conclusion:

1. Plate-FDLPA which is very similar to wire-FDLPA can be realized by using metal plate of constant thickness, by carefully choosing the width & gap for the folded dipole.
2. Use of truncation constants & the shorting stub on the longest element further helps in improving impedance matching.
3. Constant width stripe line feeding throughout the array helps in impedance matching.

9. Eleven Feed

Conventional log-periodic arrays give radiation in endfire direction coming out of the apex of the array. But Eleven Feed which is a combination of log periodic folded dipole arrays ,gives broadside radiation. This is desired to use it as a feed for the reflector while retaining the broadband characteristics of log periodic arrays.

If two dipoles are made parallel at certain height above the ground plane, and fed in phase, they give broadside radiation as discussed in chap. 3. Eleven feed uses the same concept but extend it by replacing dipoles with log-periodic arrays of folded dipoles, thus achieving broadband performance. Pattern then depends upon the separation between two parallel folded dipoles and height above the ground. Eleven feed developed by Olsson R. & Kildal P.S.[1][2][3] uses half wavelength (0.5λ) separation between folded dipoles & Height of 0.16λ above the finite square ground plane of $0.88\lambda_{max}$ width.

This clearly indicates that apart from optimization parameters of Plate-FDLPA, Eleven feed requires additional parameters like distance of folded dipoles from the symmetry plane(DP), Height above ground plane (H) & Width of ground plane (WG). Height can be equivalently expressed by making use of elevation angle Ψ made by the array with ground plane at the center and they are related as:

$$\tan(\Psi)=\frac{H}{DP} \qquad .....(9.1)$$

Eleven feed is usually enclosed in a metal box, by making vertical walls of metal on the edges of the ground plane. Usually height of these walls is the height where the axis of the array will intersect the vertical plane passing through the edge of the ground plane. But this can be additional parameter required for the design. Fig 9.1 shows such Eleven Feed Geometry in WiPl-D software. Only one quarter structure is created in WiPl-D and complete structure is simulated by making use of symmetry & antisymmetry planes. But only one polarization is simulated at once.

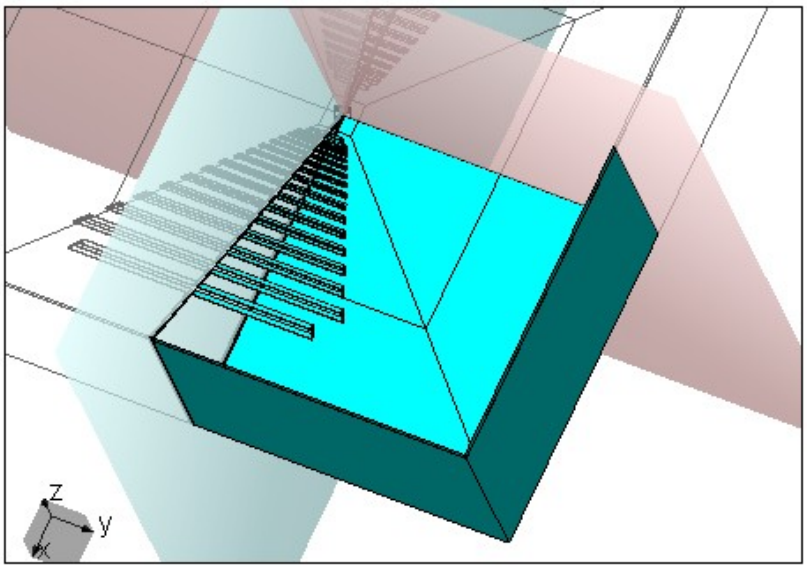

Fig 9.1 Eleven Feed Geometry in WiPl-D

Apart from these, there are additional design parameters for better impedance matching of the Eleven feed. To match Eleven feed to 50Ω, the plate FDLPA is designed for 200Ω of impedance, thus when two such arrays are connected in parallel to a coupled stripe line parallel to the ground the effective impedance is 100Ω in odd mode, thus giving 50Ω of impedance on each stripe of the coupled stripe line with respect to ground. This puts a constraint that the coupled stripe line parallel to the ground should have characteristic impedance of 100Ω which depends upon its height above the ground plane. So this is considered as additional design parameter. The complete list of optimization parameters is given in Table 9.1 and fig 9.2 shows the pictorial representation of some of the parameter.

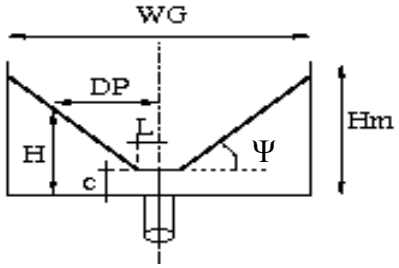

Fig 9.2: Eleven Feed Parameters (DP,H,L,c,WG,Hm)

Thus each polarization comes with two outputs, one from each stripe line parallel to ground. To excite odd mode in the structure, the 180° Hybrid is then used to combine output from these two ports, thus giving difference between the two outputs. Similar arrangement is required for orthogonal polarization as well.

Table 9.1: Complete List of Optimization Parameters

1	f_{min}	: Lowest Geometrical Frequency (Hz)
2	N	: Number of elements in an array.
3	τ	: Scaling Factor (<1)
4	σ	: Spacing Constant (<1)
5	*l*	: Length of folded dipole from antisymmetry plane (λ)
6	w_1	: Width of plate at port 1 of folded dipole (λ)
7	w_2	: Width of plate at port 2 of folded dipole (λ)
8	w_3	: Width of shorting plate (see fig 8.1) (λ)
9	g	: Gap between two parallel plates of folded dipole (λ)
10	K1	: Low Frequency Truncation Constant
11	K2	: High Frequency Truncation Constant
12	S	: Length of shorting stub on longest folded dipole (λ)
13	fg	: Width of feedgap for all folded dipoles (mm)
14	ws	: Width of stripe feeding all folded dipoles (mm)
15	t	: Thickness of the metal plates (mm)
16	DP	: Distance of folded dipoles from symmetry plane (λ)
17	Ψ	: Elevation angle of FDLPA (Degrees)
18	c	: Height of the stripe parallel to the ground (mm)
19	L	: Length of stripe parallel to the ground (mm)
20	WG	: Width of square ground plane (λ_{max})
21	Hm	: Height of metal walls from feed enclosure (m)

The entire Eleven Feed can be fully described by these 21 parameters only. Out of these 21 parameters, first 5 comes from conventional dipole log periodic arrays, parameters 6 to 12 mainly decides the widths & gaps of Plate-FDLPA. Parameters 13 to 15, comes from stripe line studies which decides characteristic impedance (200Ω) of the parallel plate line feeding all folded dipoles. Parameters 16,17 places two plate-FDLPA parallel to each other in Eleven Feed configuration; 18,19 are used to create a coupled stripe line above ground plane with 100Ω characteristic impedance. And Finally parameters 20,21 decides the size of the box enclosing the Eleven Feed. Parameter 20 (WG), decides the aperture efficiency. Olsson et.al.[1] proposes width of ground plane to be $0.88\lambda_{max}$ which gives ~-2.2dB of aperture efficiency for $\theta_o=60^o$.

Though these 21 parameters completely describe the feed geometry and have effect on its performance, determining these 21 numerical values is more an art than science!

References:

[1] Olsson R., Kildal P.S., Weinreb S., "The Eleven Antenna: A Compact Low-Profile Decade Bandwidth Dual Polarized Feed for Reflector Antennas", IEEE Trans. Antennas & Propagation, vol. 54, No.2, February 2006.

[2] Olsson R., Kildal P.S., Weinreb S., "Measurements of a 1 to 13 GHz Model of a Dual Polarized Low-Profile Log-periodic Feed for US-SKA", IEEE Symposium Antennas & Propagation, July 2005.

[3] Olsson R., Kildal P.S., Weinreb S., "A Novel Low-Profile Log-periodic Ultra Wideband Feed for Dual-reflector Antenna of US-SKA", IEEE Symposium Antennas & Propagation, June 2004.

10. Optimized Eleven Feed for GMRT

Eleven feed for GMRT has been designed for 200-800MHz frequency band with metal box size of 1.46 x 1.46 x 0.5m. For 200-800 MHz band the feed has been actually designed with 175MHz to 1131.42MHz as geometrical lowest & highest frequencies with 16 folded dipoles in each LPA.
To save computation time, only the one quarter of the feed structure is modeled in WiPl-D software, based on various parameters describing the feed geometry. The simulation results are impedance values and radiation patterns of the feed.
The amount of time required to compute one Frequency point is ~ 6 mins. For better understanding of the behavior of the feed, simulation is done with 10MHz frequency step in the desired band of interest. Figure 10.1 shows the Geometrical model of one polarization in WiPl-D software. The finite conductivity of Silver is also included for all metallic part of the structure.

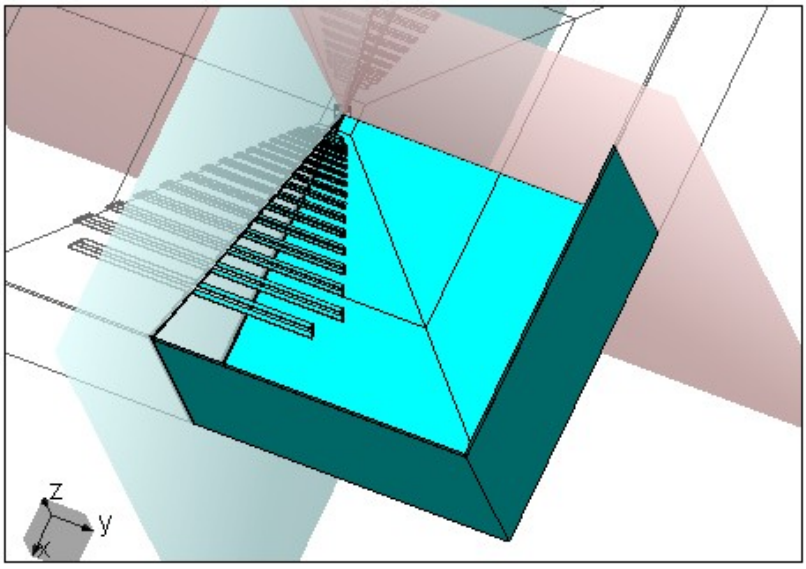

Fig 10.1: Geometrical Model in WiPl-D

From WiPl-D simulation we get antenna impedance and radiation patterns. These values are read in Matlab and scripts are written to compute all feed sub-efficiencies from these radiation patterns and impedance values. On subsequent pages the plots are given describing the feed performance for GMRT dish which has half subtended angle of 62.5 degree. The results are computed for 63 degree half subtended angle of the reflector.
For this feed, the shorting stub (see fig 10.2) on the last folded dipole is connected to the vertical wall of the metal box, thus giving thermal conductivity in entire structure. Also in order to make manufacturing easy, Plate-FDLPA are first cut from stainless steel plates of 2mm thickness with LASER cutting. After cutting, Silver with thickness of 3 times the skin depth at 170MHz is chemically deposited on stainless steel.
For support structure low loss Rohacell Foam is used which has dielectric constant of 1.001. This dielectric support is not modeled in WiPl-D since it has very low loss.

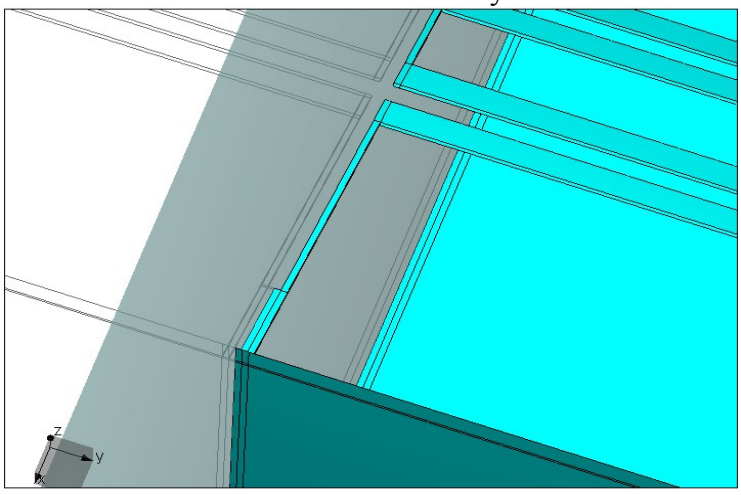

Fig 10.2: Shorting Stub on Last Folded Dipole

The Center part of the feed, including the transition from strip line to coax lines is machined separately. And then joined to the strip lines of folded dipole with additional top plate of same width & thickness. This overlap (see fig 10.3)has also been modeled in the WiPl-D to understand its effect on S11.

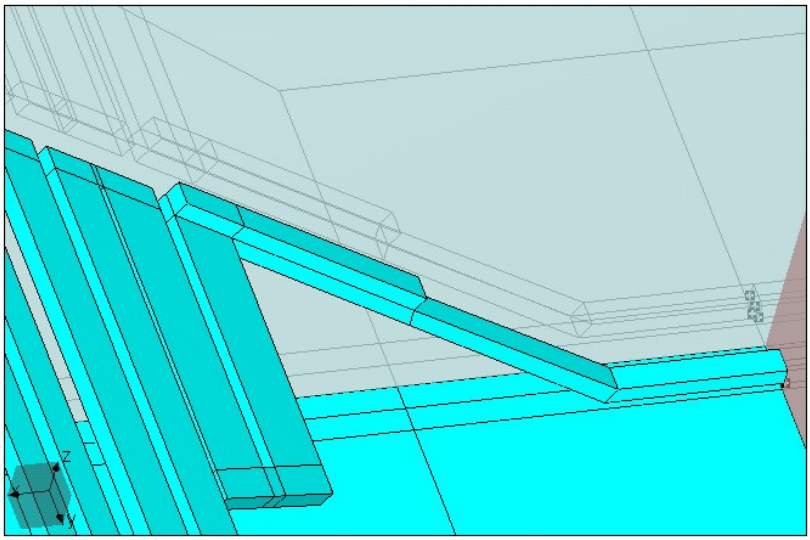

Fig 10.3: Overlap on Strip Line

The orthogonal polarization is also simulated in similar manner with only difference in the height of stripe at the center & its length such that stripes for both polarization can exists at the same time without intersecting each other.

The complete list of parameter values used for this design in given in Table 10.1.

Table 10.1: Numerical values of Optimization Parameters

f_{min} =175MHz	N=16	τ = 0.883
σ = 0.055	l = 0.232	w1 = 0.01
w2 = 0.01	w3 = 2mm	g = 0.008
K1 = 0.80	K2 = 0.80	S = 0.0182
fg = 6mm	ws = 3mm	t = 2mm
DP = 0.25	Ψ = 33^o	c = 5mm
L = 15mm	WG= 1.46m	Hm = 0.5m

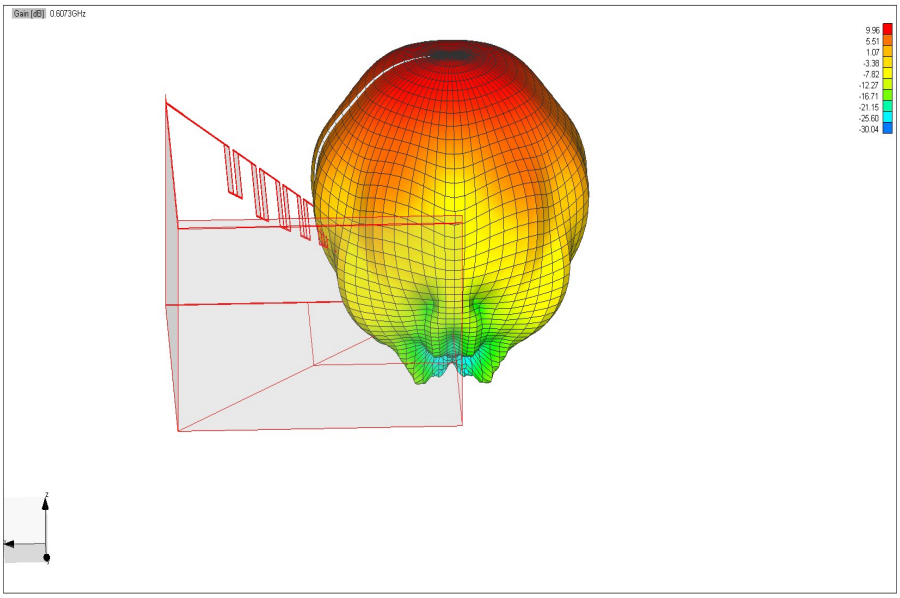

Fig 10.4: Radiation Pattern at 607MHz

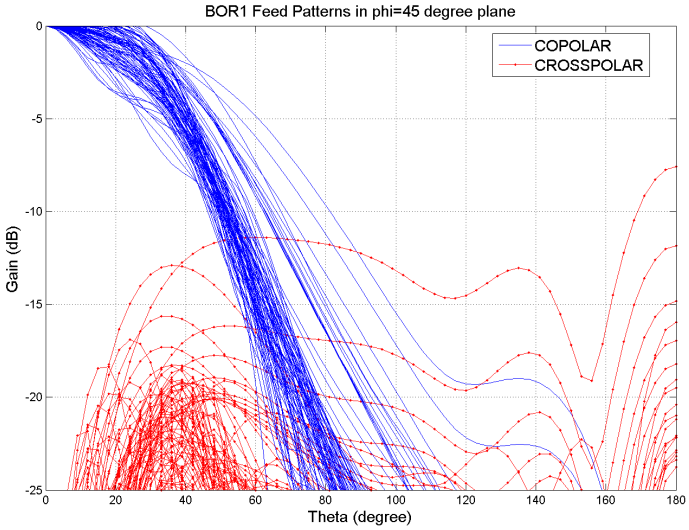

Fig 10.5: Copolar & Crosspolar BOR1 patterns

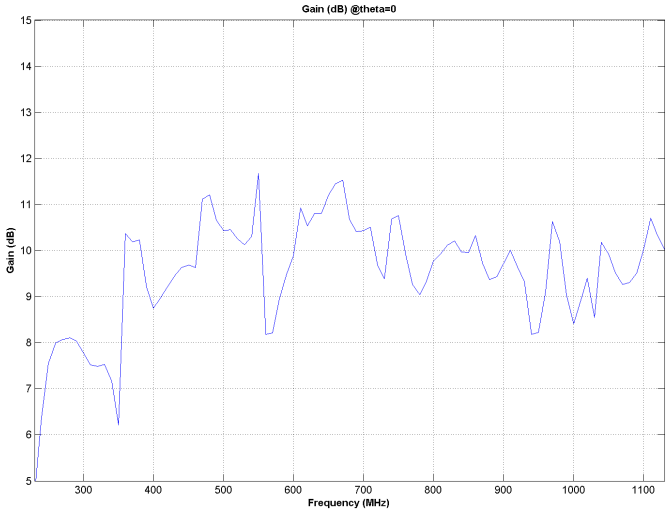

Fig 10.6: Variation of Gain with Frequency

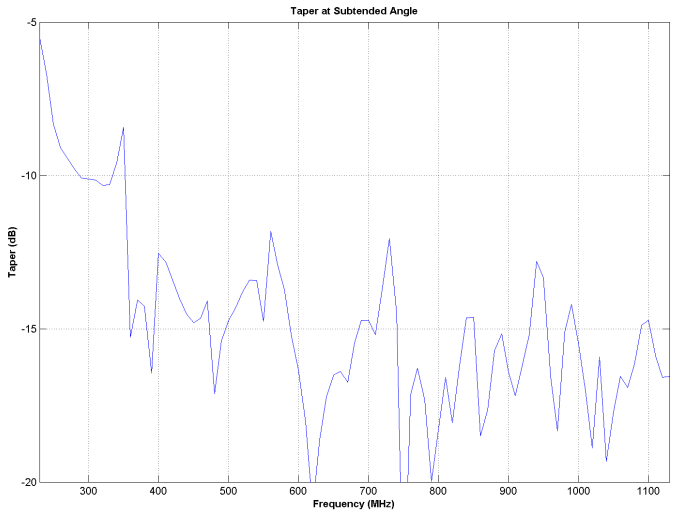

Fig 10.7: Taper of BOR1 components at 63°

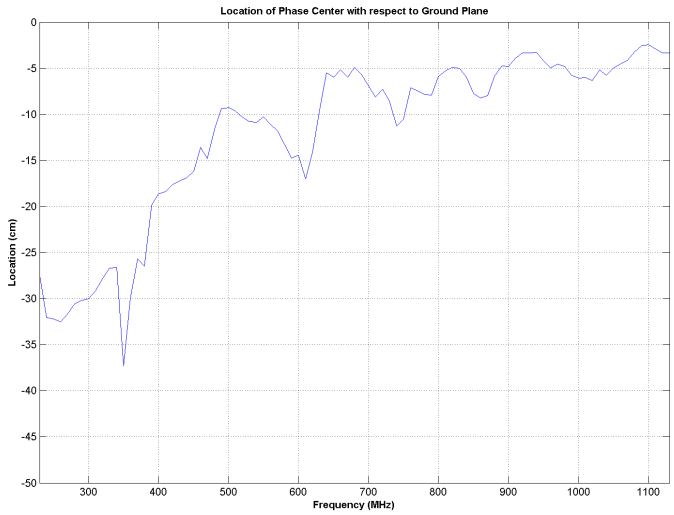

Fig 10.8: Variation of Phase Center

Note:- The optimum phase center is assumed to be 5cm below ground plane for all frequencies.

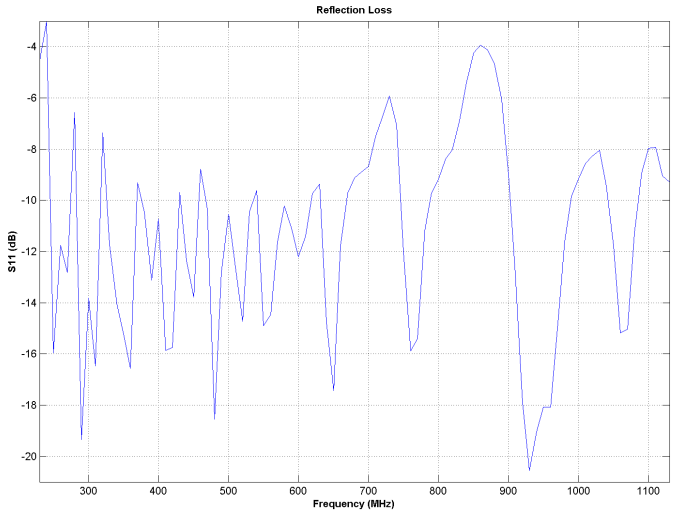

Fig 10.9: Input Reflection Coefficient

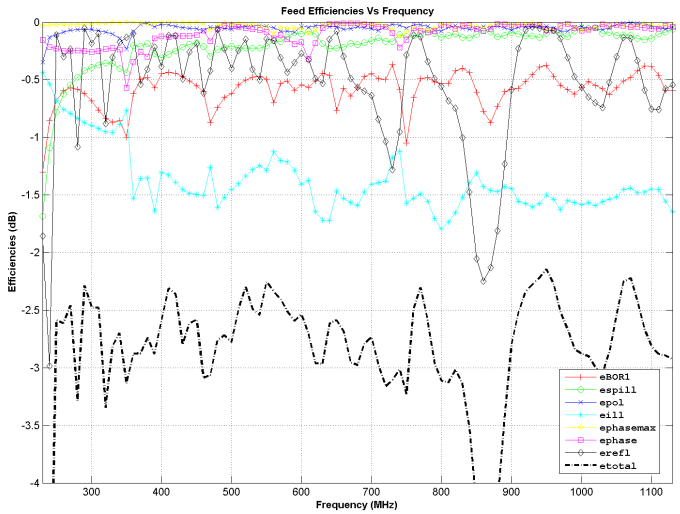

Fig 10.10: Feed Sub-efficiencies

Advantages of this Design:

- Eleven Feed is fully described by 21 parameters only.
- Performance of Eleven feed depends only on these 21 parameters, and it can be improved by careful choice of these parameter values.
- Reflection loss has been improved from prior designs. S11 is less than -10dB over 80% of the band.
- The total feed efficiency is -3dB or better over large part of the band.
- The aperture efficiency is ~ -2.2dB for 63^{o} half subtended angle of GMRT reflector.
- Peak crosspol level is -15dB or less in total pattern, while it is -20dB or less in BOR1 patterns giving polarization efficiency of ~ -0.1dB.
- No manual tunning is done to any of the feed dimensions.
- Shorting stub on last folded dipole is joined to wall of the metal box, thus there exists thermal conductivity in entire feed structure, which is helpful for cooling purposes.

Disadvantages:

- Still to improve S11. The reason of higher impedance variations at higher frequencies is not clear yet.
- The strip lines feeding the folded dipoles are too thin as compared the the dimensions of the dipoles. So additional support structure is required to support dipoles.
- The additional support structure made up of Rohacell is not included in modeling which will have effect on reflection loss.
- Orthogonal polarization is not included in the modeling. Stripes for orthogonal polarization will effect on reflection loss.
- Still to improve peak crosspol level.

11. Crosspol PINs
Innovative Concept to Reduce Crosspol

In Eleven Feed the peak cross-polar side lobe is ~ -16dB w.r.t to co-polar maximum. In order to reduce this level, it is important to understand which part of the structure are more sensitive to crosspol.
On the basis of simulations with different widths & gaps of folded dipole in basic Eleven configuration as shown in fig 11.1, author proposes that the crosspol level increases with increases in width of radiating plates & shorting plate of the folded dipole. i.e. (w1,w2,w3). To achieve more bandwidth out of single folded dipole usually the widths are made larger but it increases crosspol. So crosspol & bandwidth seems to be trade off.

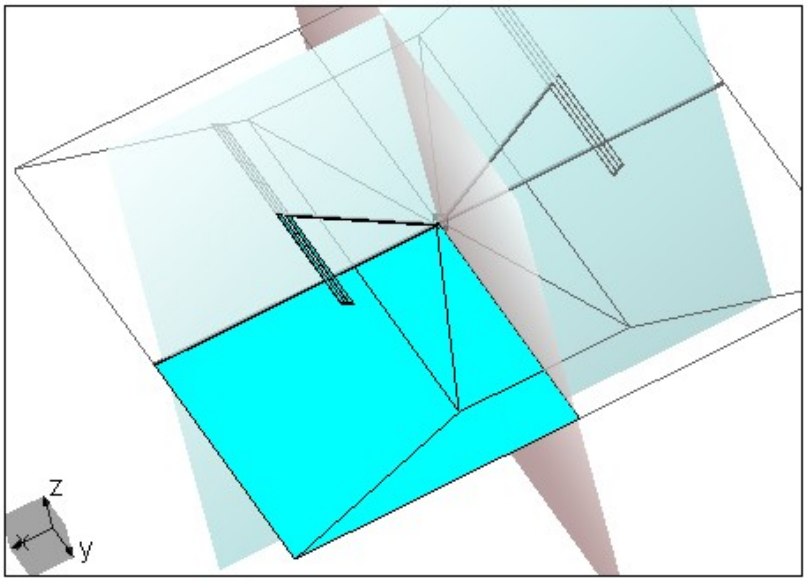

Fig 11.1: Conventional Folded Dipole in Eleven Configuration

To improve this, author has invented a new parasitic element which is made up of wire with inverted 'U' shape closely coupled to the short edge of folded dipole and shorted to the ground plane as shown in fig 11.2.

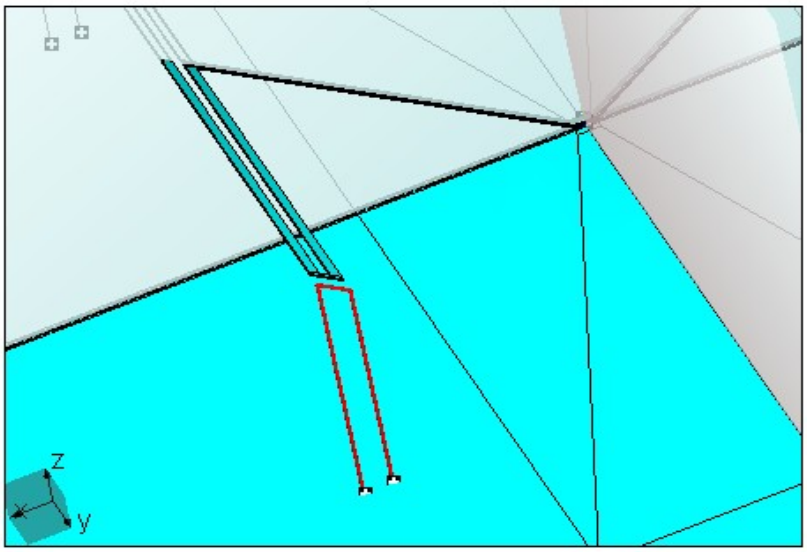

Fig 11.2: Crosspolar PINS

Fig 11.3 & 11.4 gives the 3-D radiation pattern simulated in WiPl-D software for normal case of fig 11.1 & for Crosspolar Pins of fig 11.2. For normal case the Gain on axis is 10.02dB with peak cross polar level of -8.57dB, this giving -18.59dB of peak cross polar side lobe. But with use of Crosspolar PINS, the peak crosspolar side lobe is reduced to -22.95dB, which is significant ~4.5dB improvement in crosspolar level.

For the Crosspolar PIN shown in fig 11.2, the radius of wire used is 2mm, while its offset from the short edge of the folded dipole is 15mm. The peak crosspolar level is a strong function of these two variables. Also it has an effect on impedance matching as shown in fig 11.5

At this stage, this parasitic element is not investigated in detail. But certainly it has many aspects to study in depth, like its effect on matching, bandwidth etc. If this concept is working for single Folded Dipole in Eleven Configuration, then putting such PINS on all folded dipoles in Eleven Feed may significantly improve its crosspolar performance. But more work is required to comment further on this topic.

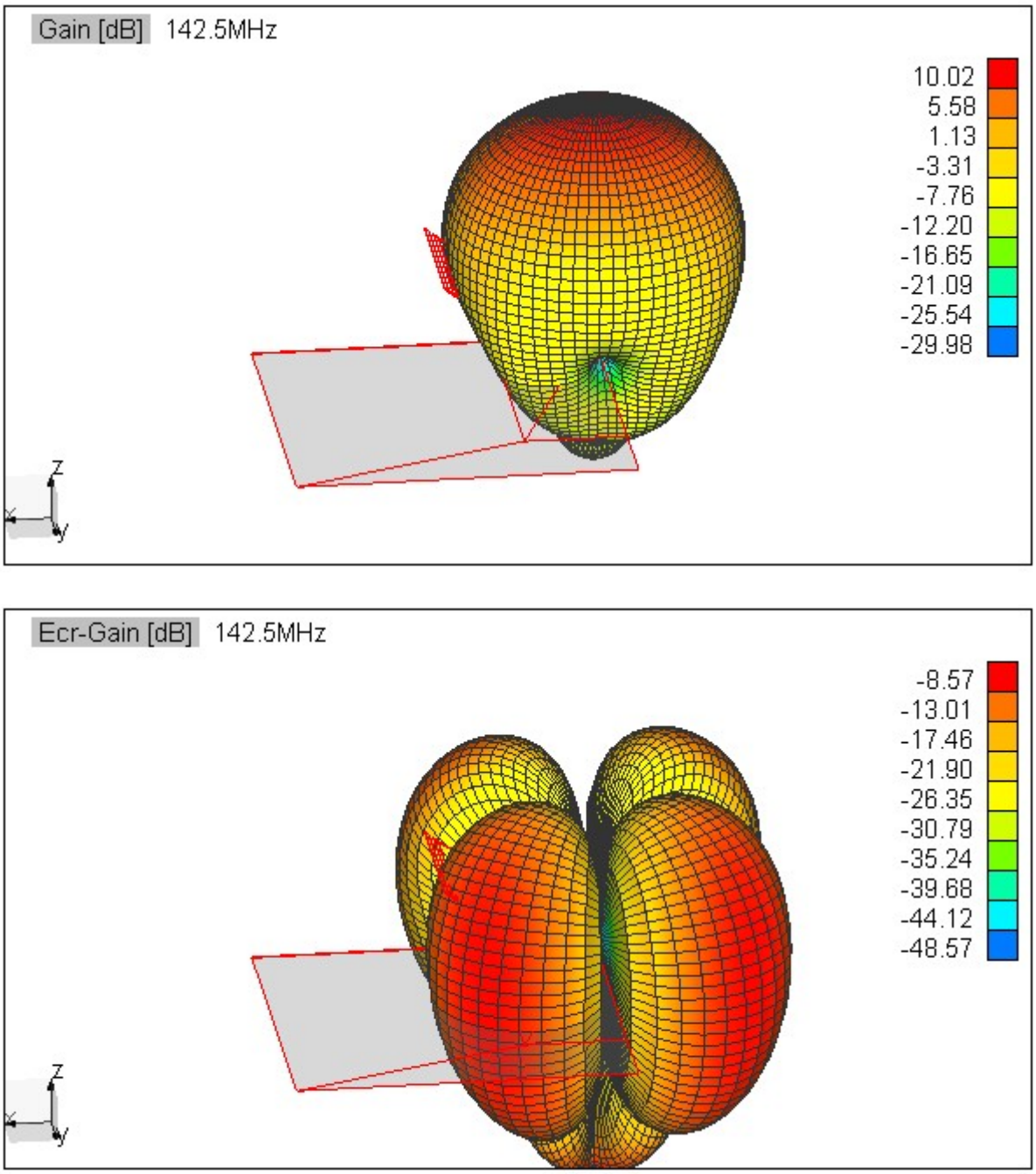

Fig 11.3: Copolar & Crosspolar 3-D patterns without PIN

From Fig 11.3, peak crosspolar level with respect to peak copolar is -18.59dB.

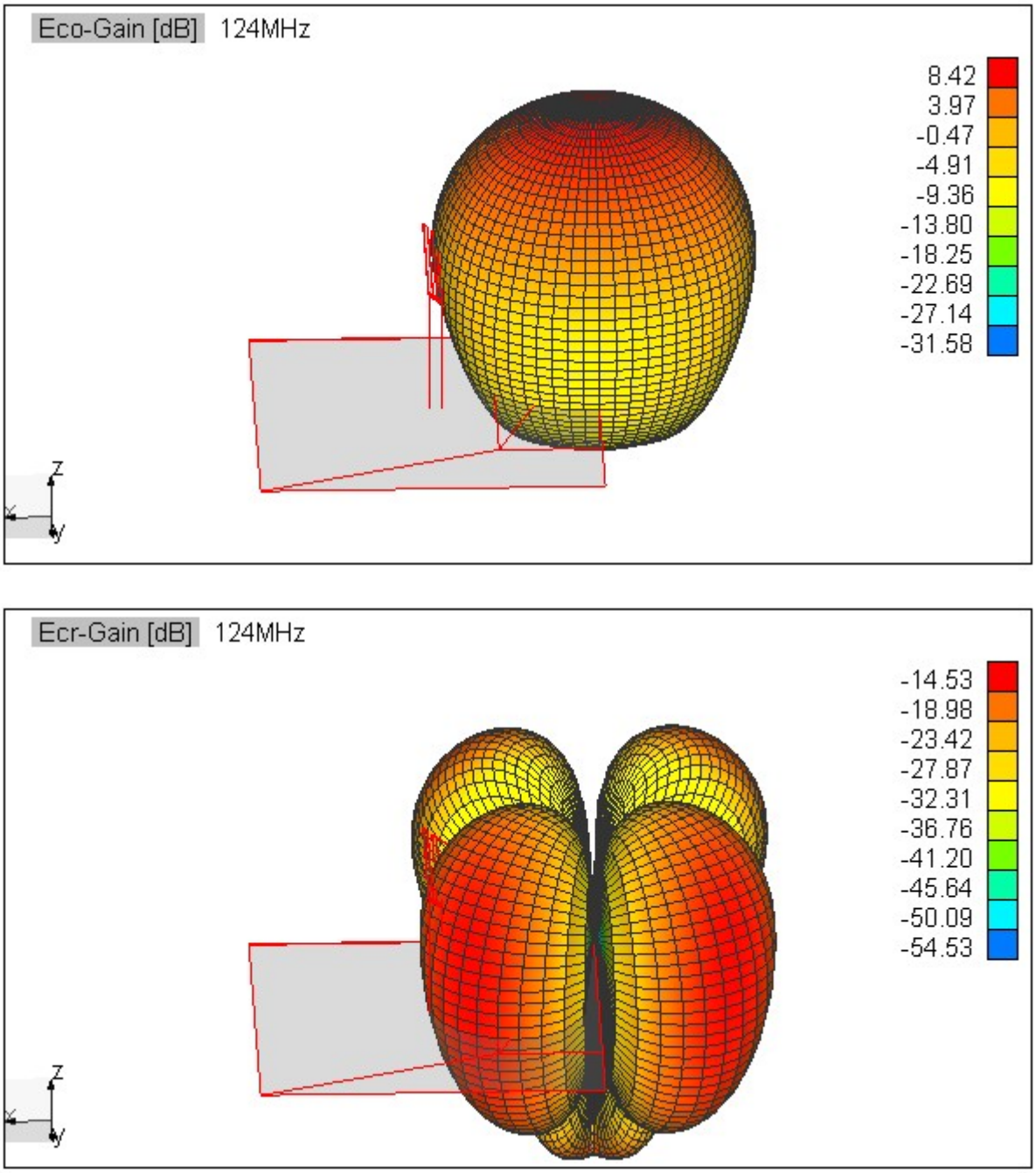

Fig 11.4: Copolar & Crosspolar 3-D patterns with PIN

From Fig 11.4, peak crosspolar level with respect to peak copolar is -22.95dB. Thus by putting XP PIN the peak crosspolar is reduced by factor of 5dB, which is significant improvement.

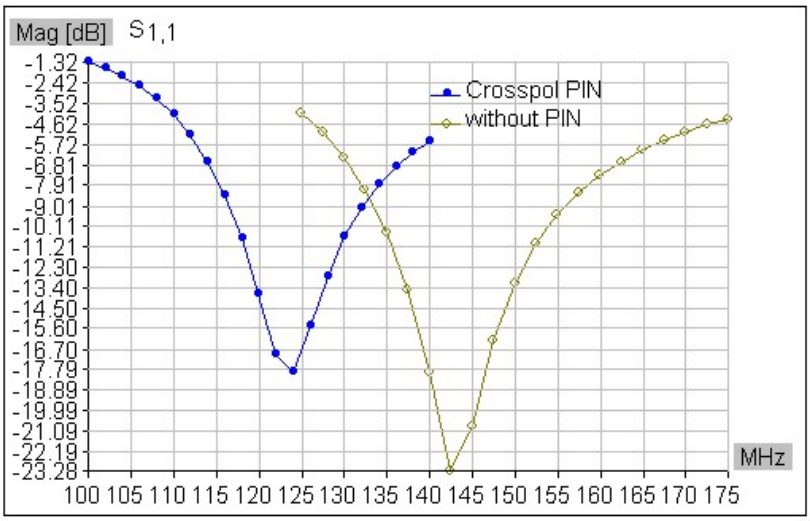

Fig 11.5: Effect of PIN on Impedance Matching

Table 11.1: Optimization Parameters values

f = 150MHz	*l* = 0.23	w1=w2=0.008
g = 0.008	fg = 6mm	ws = 3mm
t = 2mm	DP = 0.24	H = 0.18
c = 5mm	L = 15mm	WG = 1

12. Conclusion
&
Further Work

Conclusion:

Eleven Feed is an excellent concept to get broadside radiation by making use of two parallel folded dipole log-periodic arrays above a ground plane giving decade bandwidth. This makes Eleven Feed suitable for wide band feed for the reflector since there is very less variation of phase center.

Pattern of the Eleven Feed & hence aperture efficiency depends upon the distance between two parallel dipoles, height above the ground plane & the size of square ground plane.

For Impedance matching, the conventional log periodic array techniques are applicable to Eleven Feed as well. Better reflection loss can be achieved by careful design of Plate-FDLPA used in Eleven Feed. Use of constant characteristic impedance transmission line, truncation constants & shorting stub further improves the impedance matching.

Optimized Eleven Feed for GMRT, improves S11 to -10dB or less over large part of the band as compared to -6dB or less for the prior versions of Eleven Feed.

The Eleven Feed has a gain of ~11dB for most of the frequencies. This gain is bit more than required since the GMRT dish is a deep paraboloid with θ_o of 62.5^o, this causes the reduction in Illumination efficiency because of high taper and dish remains under illuminated.

Still the total efficiency of the feed is ~ -3dB or better over 250 to 800 MHz band & 900 to 1100MHz. This proves its broad band performance.

Further Work:

- Understand effect of DP, Ψ & WG on pattern. And how to improve the aperture efficiency for given θ_o of the reflector by carefully choosing these parameters values?
- Extend two-port folded dipole theory to take into account the mutual coupling between folded dipoles.
- Use of this theory to analytically predict the input impedance of periodically loaded transmission line with folded dipoles.
- Analytical formulas for characteristic impedance of parallel plate strip line for given thickness, width & separation.
- Study of equivalent radius of rectangular plates.
- Further improve reflection loss with target of S11 -12dB or less.
- How to make Crosspol PINS broad band and use them on each folded dipole to reduce peak crosspolar side lobe?
- Integration of Feed with LNA & Hybrid.

Appendix A
Simulation Results for Orthogonal Polarization

Orthogonal polarization is simulated by using same optimization parameters as given in Table 11.1, with only difference in the values of c & L being 2mm & 18mm respectively. Figures below show the simulation results.

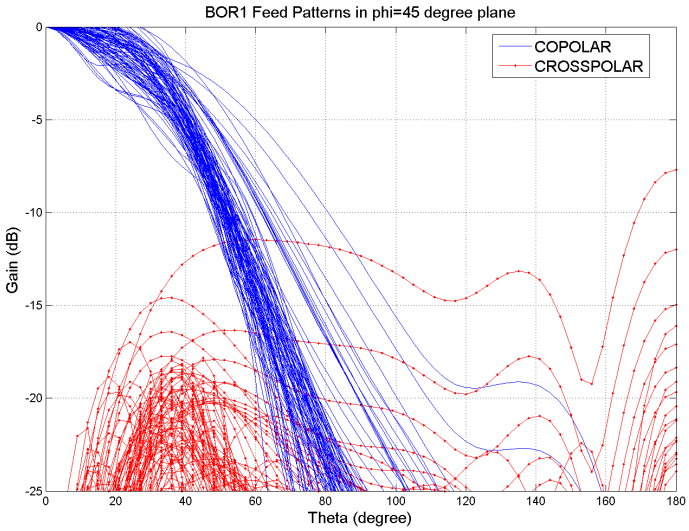

Fig A.1: BOR1 Copolar & Crosspolar Patterns

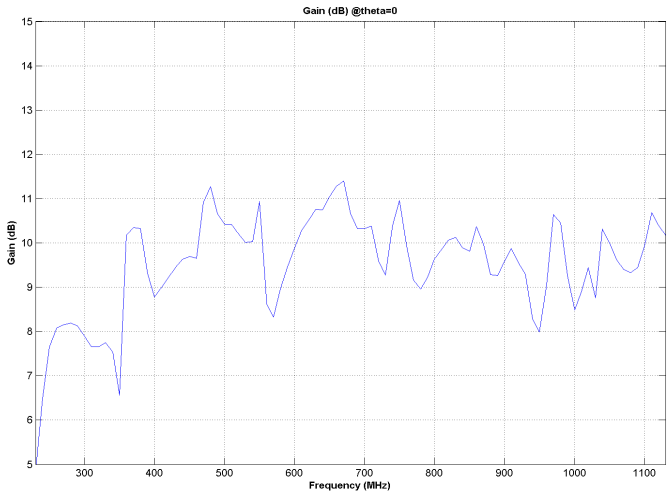

Fig A.2: Variation of Gain with Frequency

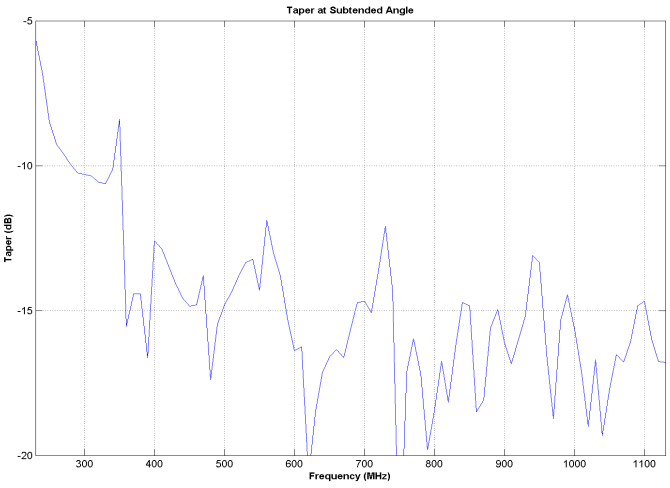

Fig A.3: Taper at θ_o=63^o of BOR1 components

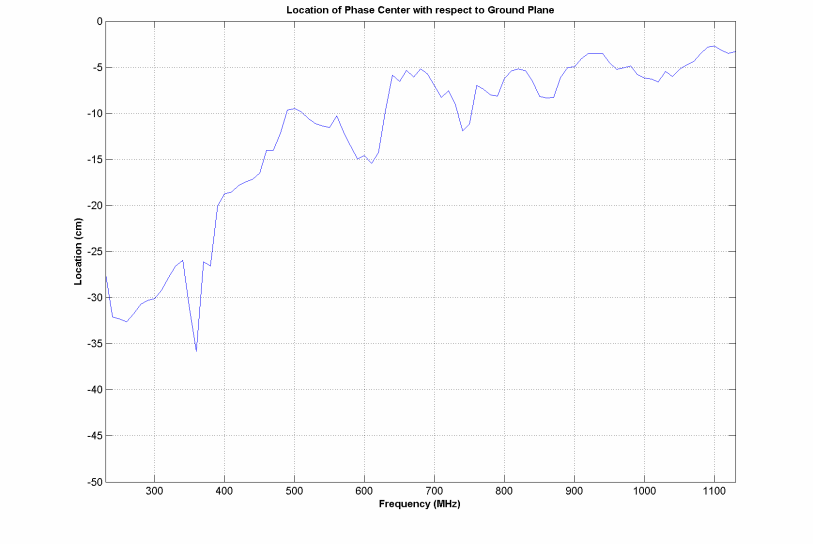

Fig A.4: Variation of Phase Center

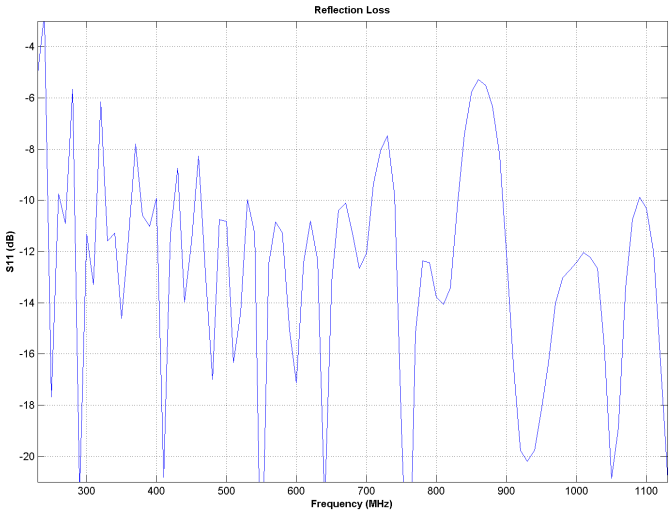

Fig A.5: Reflection Loss

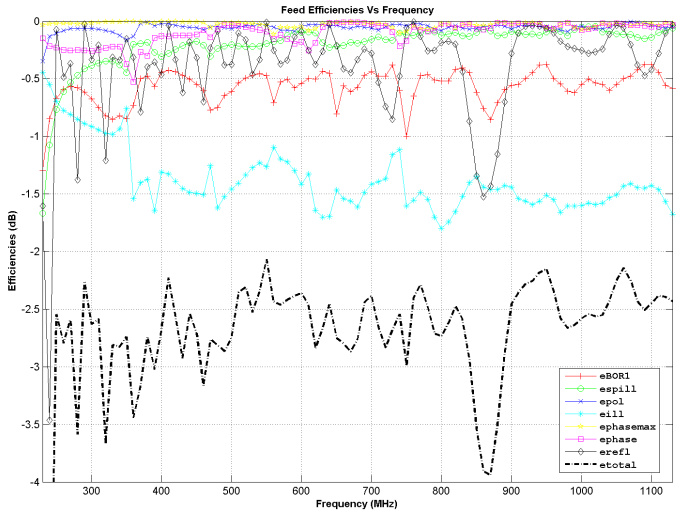

Fig A.6: Feed Sub-efficiencies.

Appendix B
Comparison Between Measurements & Simulations

Reflection Loss

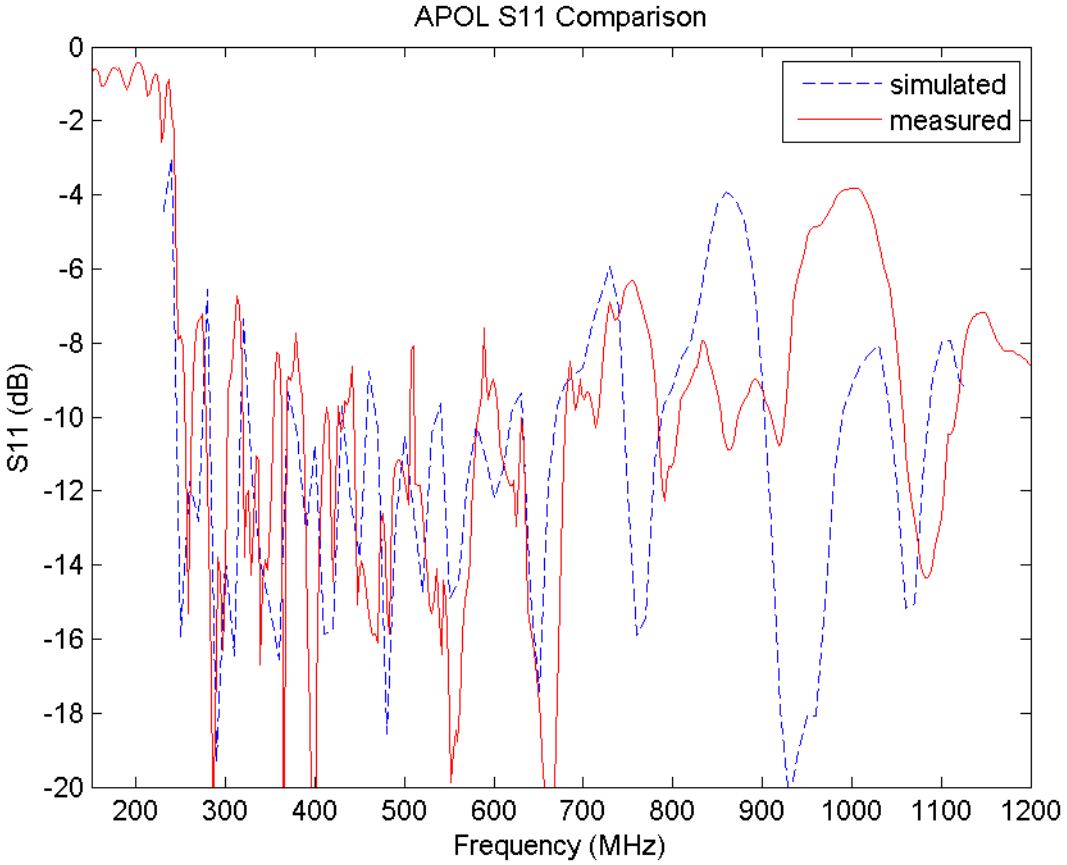

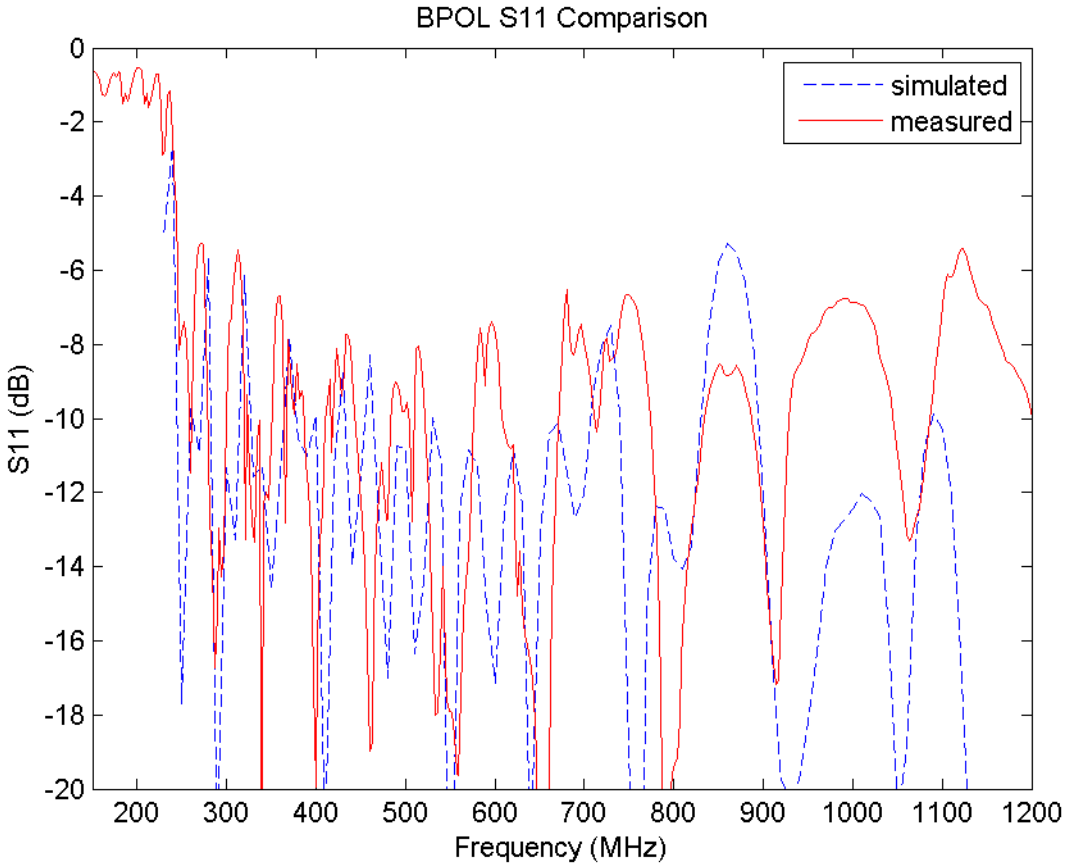

Radiation Patterns - APOL

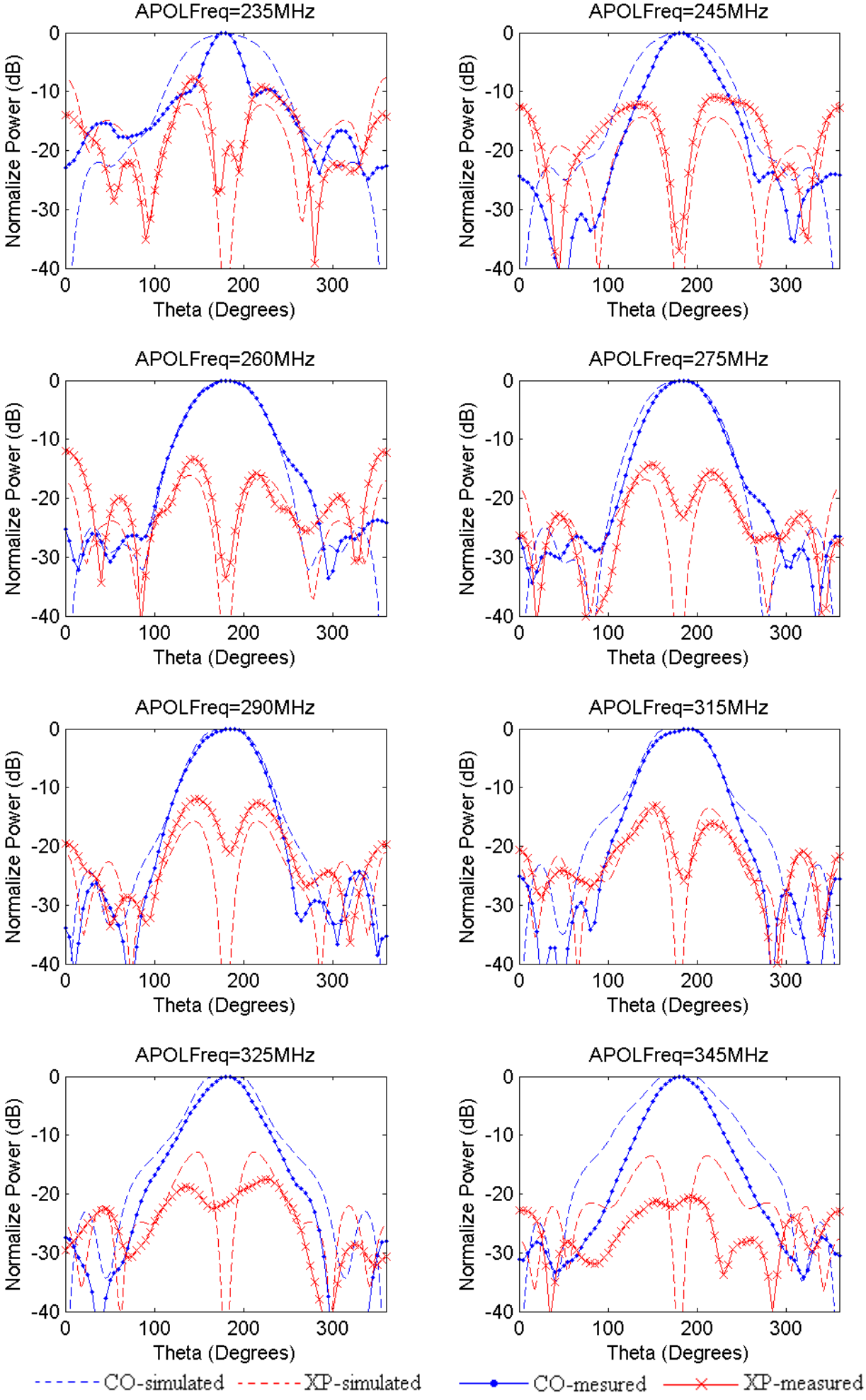

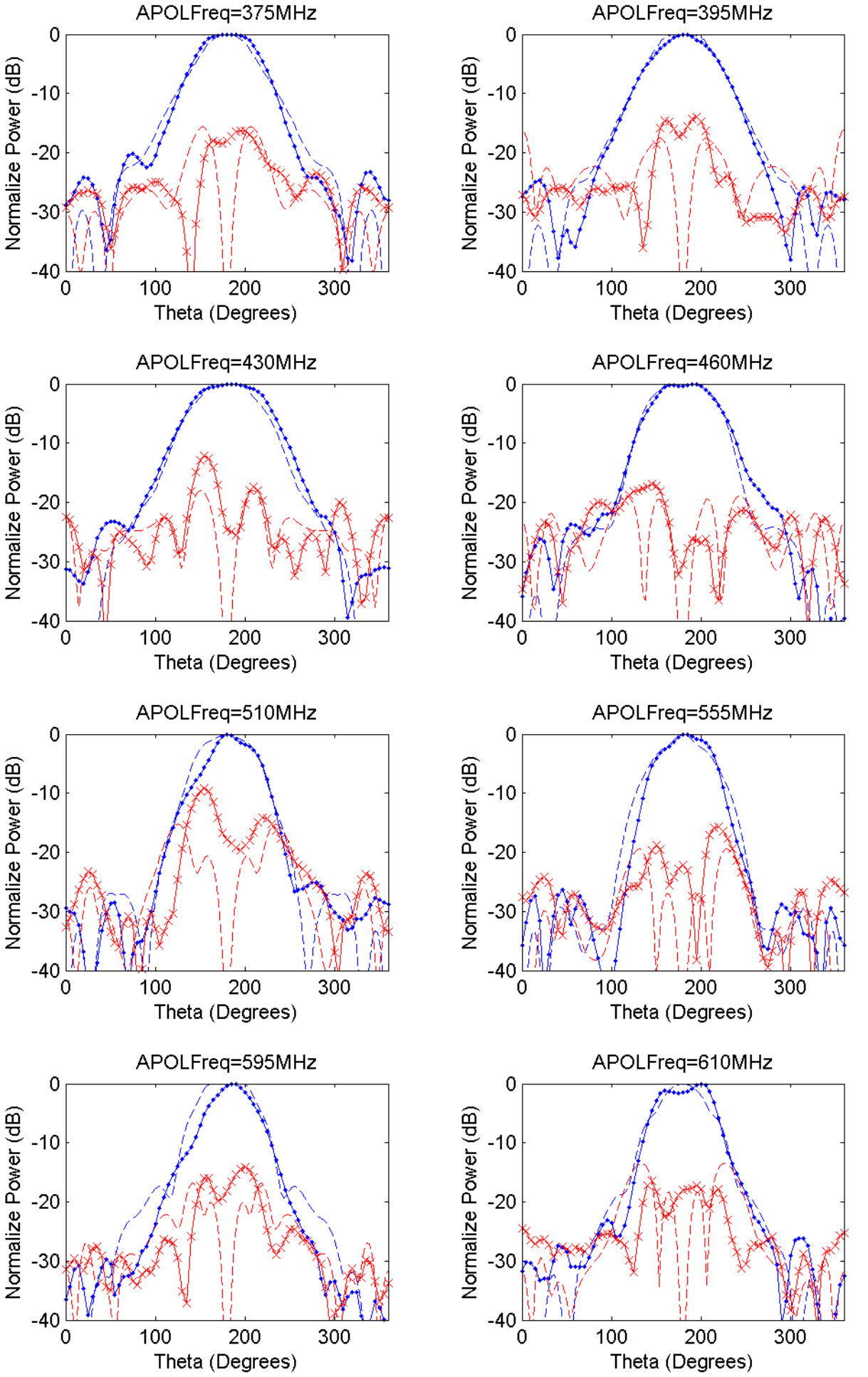
APOLFreq=375MHz
APOLFreq=395MHz
APOLFreq=430MHz
APOLFreq=460MHz
APOLFreq=510MHz
APOLFreq=555MHz
APOLFreq=595MHz
APOLFreq=610MHz
Normalize Power (dB)
Theta (Degrees)
0
-10
-20
-30
-40
0
100
200
300
CO-simulated
XP-simulated
CO-mesured
XP-measured

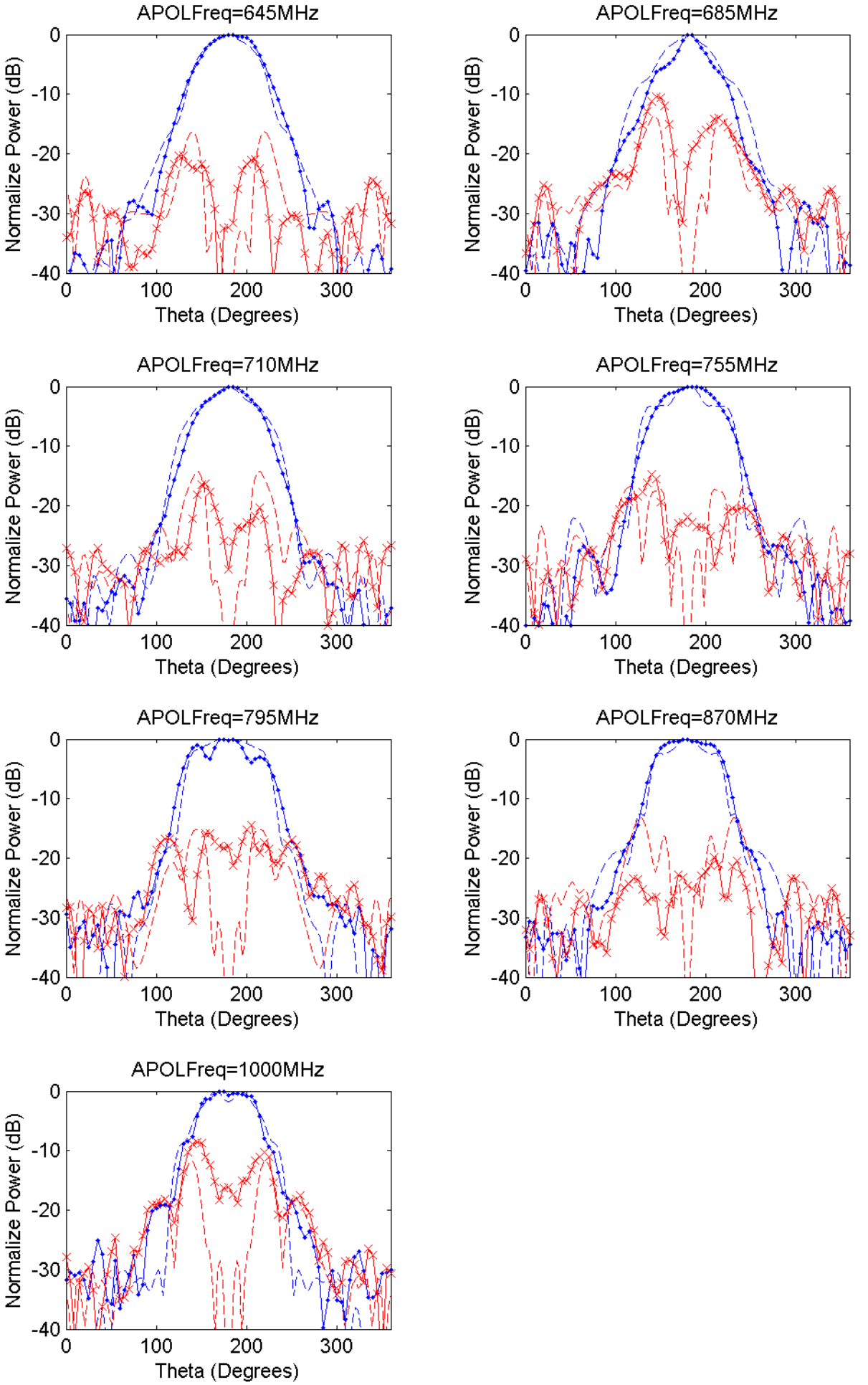
APOLFreq=645MHz
APOLFreq=685MHz
APOLFreq=710MHz
APOLFreq=755MHz
APOLFreq=795MHz
APOLFreq=870MHz
APOLFreq=1000MHz
Normalize Power (dB)
Theta (Degrees)
0
-10
-20
-30
-40
0
100
200
300
CO-simulated
XP-simulated
CO-mesured
XP-measured

Radiation Patterns - BPOL

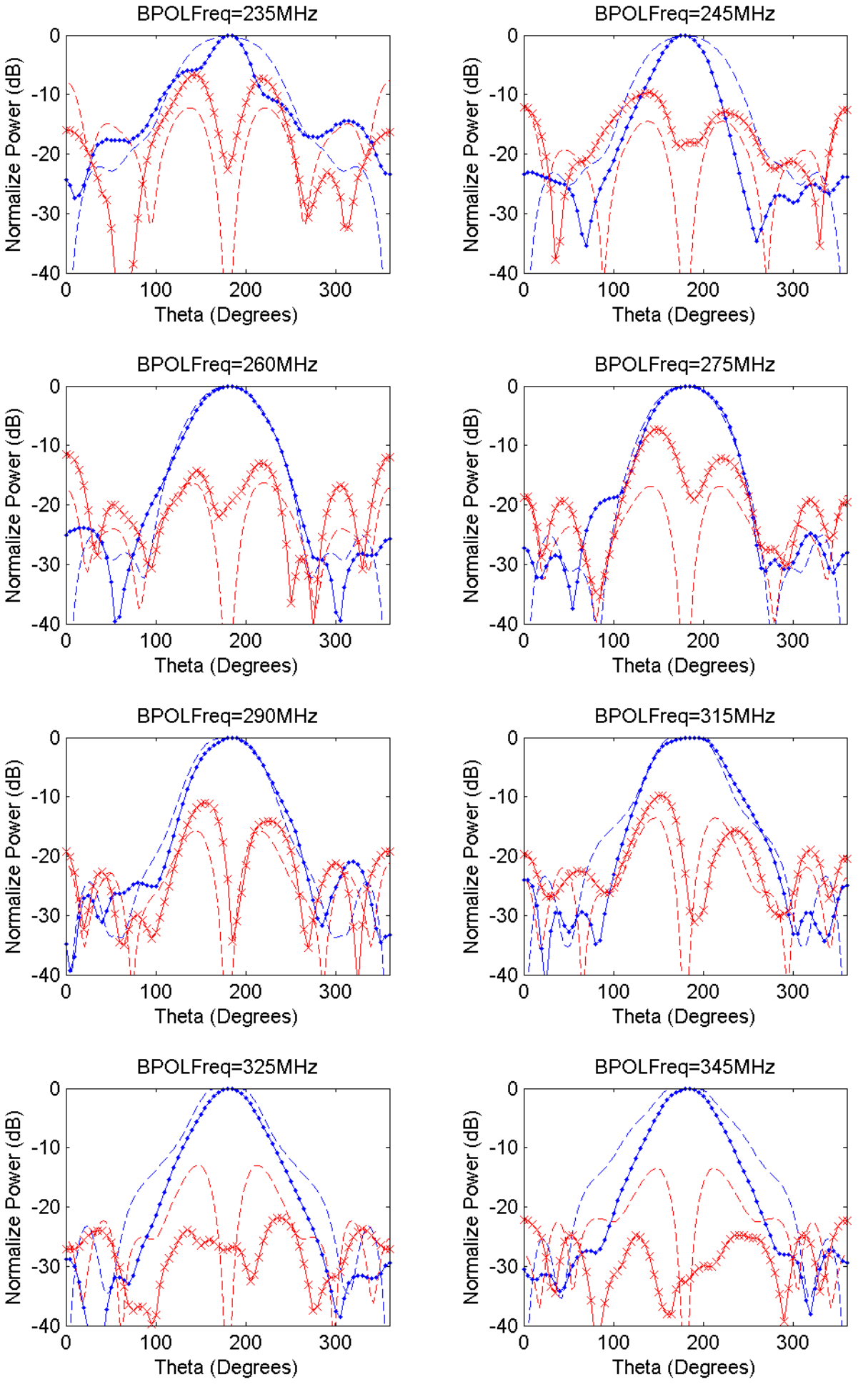

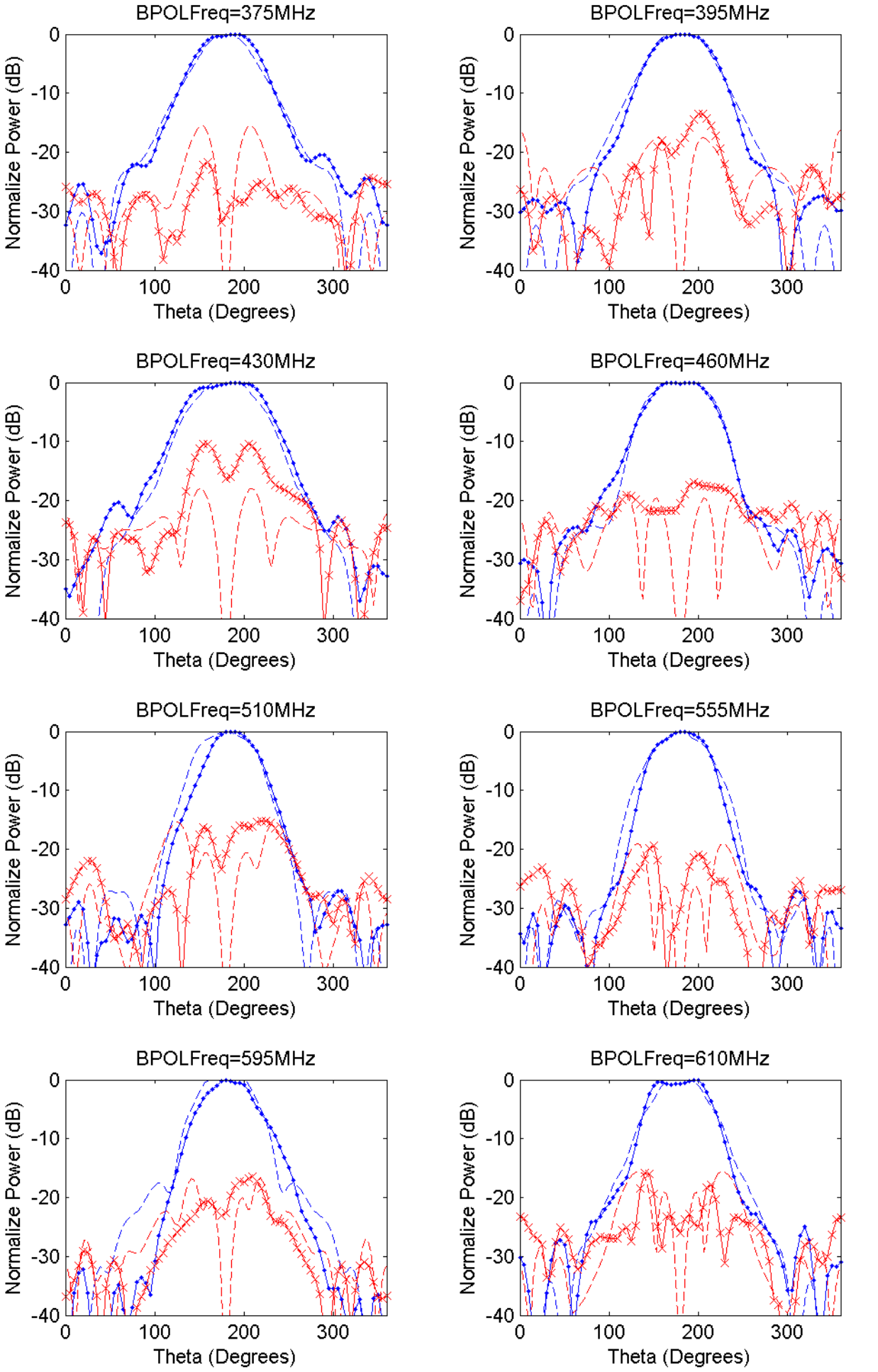
BPOLFreq=375MHz
BPOLFreq=395MHz
BPOLFreq=430MHz
BPOLFreq=460MHz
BPOLFreq=510MHz
BPOLFreq=555MHz
BPOLFreq=595MHz
BPOLFreq=610MHz
Normalize Power (dB)
Theta (Degrees)
0
-10
-20
-30
-40
0
100
200
300
CO-simulated
XP-simulated
CO-mesured
XP-measured

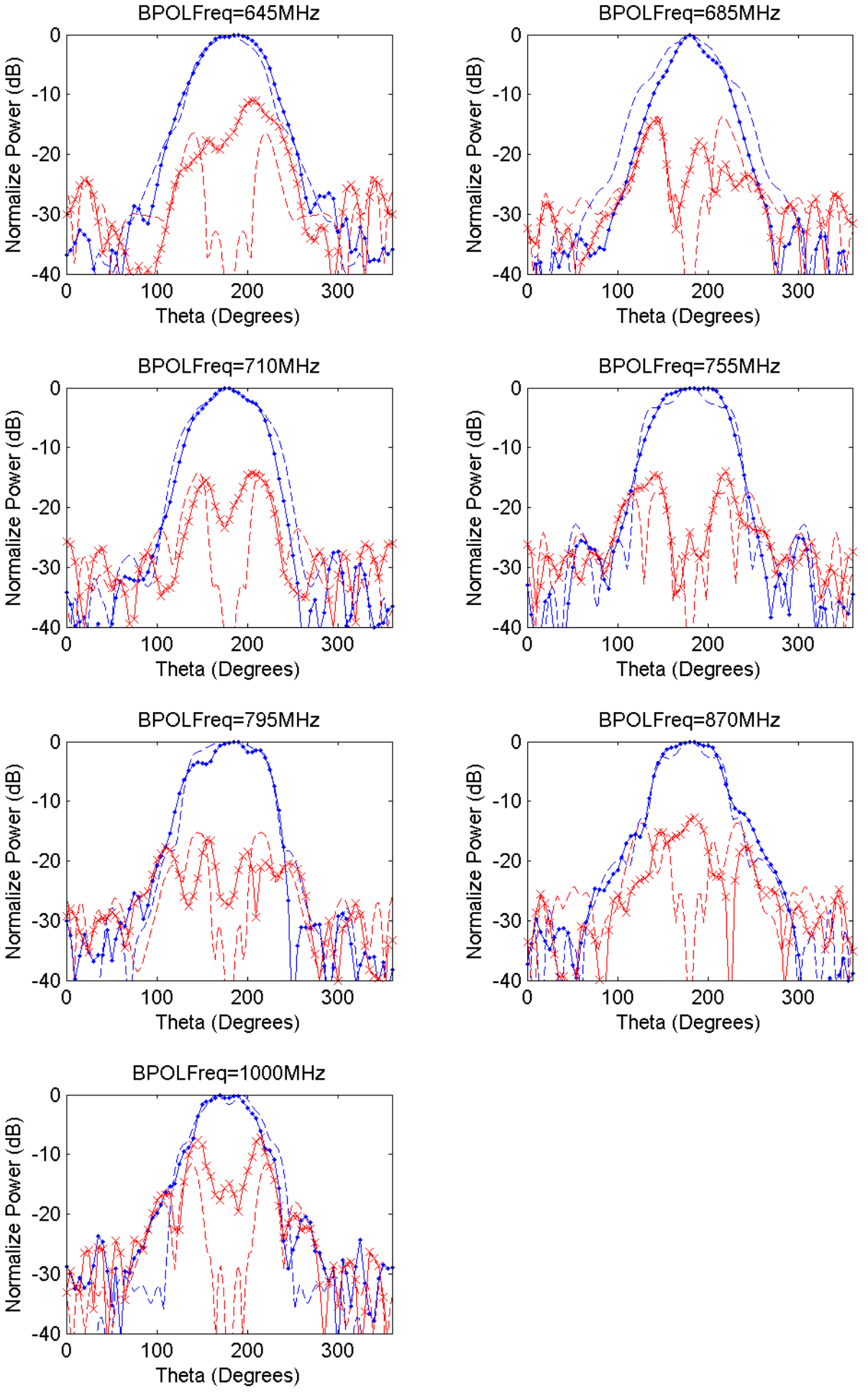
BPOLFreq=645MHz
BPOLFreq=685MHz
BPOLFreq=710MHz
BPOLFreq=755MHz
BPOLFreq=795MHz
BPOLFreq=870MHz
BPOLFreq=1000MHz
Normalize Power (dB)
Theta (Degrees)
0
-10
-20
-30
-40
0
100
200
300
CO-simulated
XP-simulated
CO-mesured
XP-measured

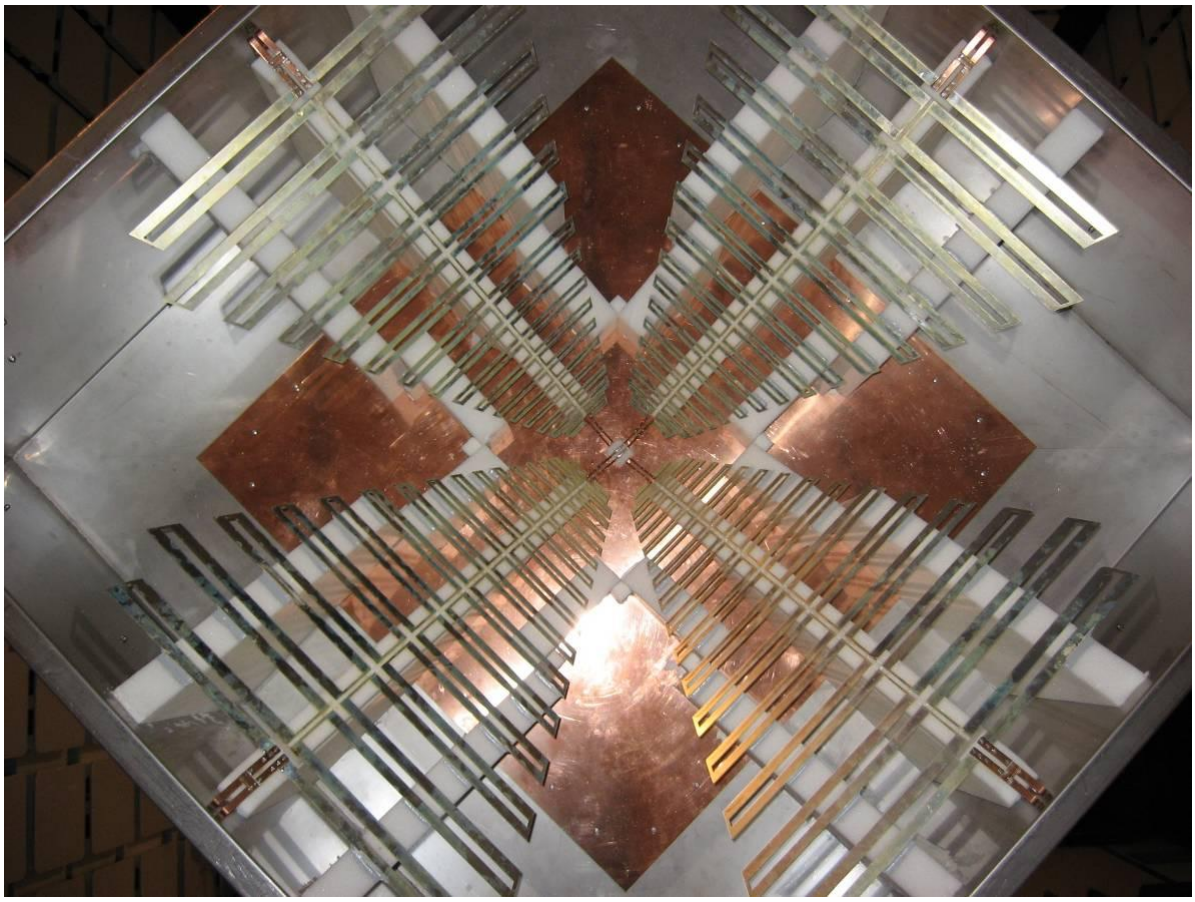

Closeup of Eleven Feed

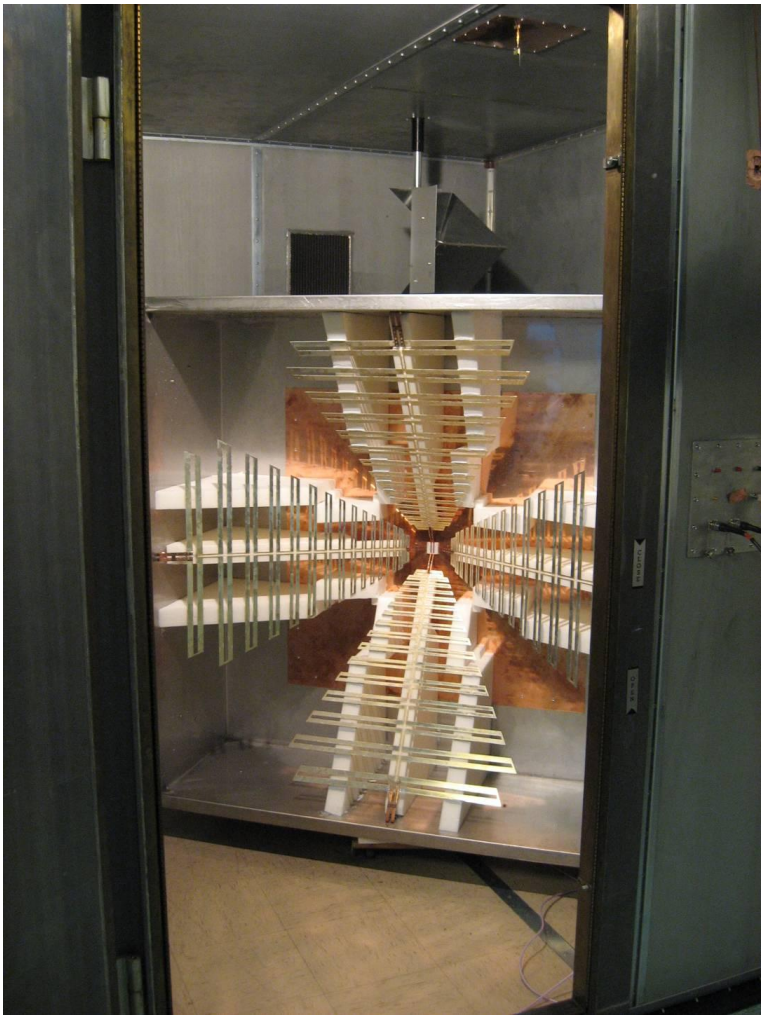

Eleven Feed in Reverberation Chamber at SP